Power and energy management of a residential hybrid photovoltaic-wind system with battery storage

by

Andreea-Cristiana Zaharof

AALBORG UNIVERSITY
DENMARK

Aalborg University

Department of Energy Technology

Group: WPS4-1050

Date: 1st of June

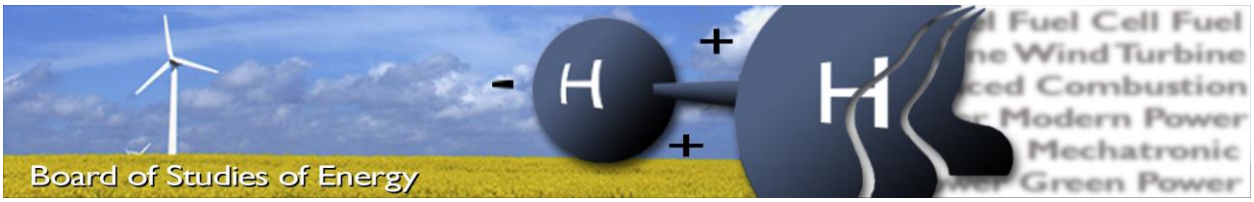

Title:	**Power and energy management of a residential hybrid photovoltaic-wind system with battery storage**
Semester:	**MSc4**
Semester theme:	**M4- Master's Thesis**
Project period:	**2nd of February - 1st of June**
ECTS:	**30**
Supervisors:	**Florin Iov, Daniel-Ioan Stroe**
Project group:	**WPS4-1050**

Andreea-Cristiana Zaharof

SYNOPSIS: With the increasing power demand and the continuously developing of renewable energy technologies, battery energy storage systems (BESS) seem to be an important part of a smart grid, providing many benefits such as reducing the electricity bill, reduction of peak demand and meeting the generation with demand side. In this study, a battery performance model is proposed for a residential home with distributed generation from renewable resources. Real irradiance and wind speed data measured in two different periods of the year (i.e. summer and winter) have been used and simulated for 24 hours. Battery storage is a suitable solution due to the fast response and flexibility. Integrated with a smoothing functionality, it can charge and discharge to reduce the power fluctuations produced by PV panels and wind turbine. Simulations show that the chosen moving average algorithm does not require a big battery size, delivering satisfactory results even with a smaller battery. Further, considering the demand power of the house and the produced power, an average power curve is computed every 15 minutes in order to be exchanged with the utility grid and minimize the electricity bill.

Pages, total:	[76]
Appendix:	[4]
Supplements:	[0]

By accepting the request from the fellow student who uploads the study group's project report in Digital Exam System, you confirm that all group members have participated in the project work, and thereby all members are collectively liable for the contents of the report. Furthermore, all group members confirm that the report does not include plagiarism.

Summary

In Denmark, municipalities started to play a more active role in supporting the energy production from renewable resources, the subsidies offered for this being in a continuous ascension. Therefore, the number of installed wind/PV systems increased and will continue to increase in the future. Moreover, the storage systems associated with photovoltaic and wind energy are a promising solution for future households, in maximizing the residential self-consumption, reducing the grid costs, power-smoothing, peak-shaving.

The current work presents a battery performance model suitable for studies related to distributed generation from renewable resources for residential applications.

A Lithium-ion battery performance model was proposed and parameterized following the Thevenin equivalent electrical circuit. The model has been validated with the experimental data conducted on the battery cell, concluding that the proposed electrical model is suitable for the studied renewable applications.

Two battery sizes are proposed for the study, a 3 kW battery and a 6 kW battery

The battery is able to compensate the high variability of the renewable resources. Integrated with a moving average functionality, it perfectly smoothens the produced power by charging and discharging following a target power given by the moving average algorithm. The simulations show that both batteries are well qualified for this application.

Further, in order to maximize the usage of renewable energy and minimize the electricity bill, a 15-minute average power curve is computed considering the house power profile and the power produced. The remained power will be charged/discharged from the battery. However, for this application a 6 kW battery is better recommended, because even when the production from renewable resources is reduced, a 3 kW battery would exceed its power limit.

Finally, the project goals have been achieved, the modeled battery energy storage system could provide suitable support for the studied renewable resources applications.

Preface

The 10th semester project was conducted at The Department of Energy Technology, Aalborg University, as a completion of the Master education in Wind Power Systems. It was undertaken and written by group WPS4-1050 during the period between 2nd of February 2017 and 1st of June 2017.

This thesis presents a battery performance model suitable for studies related to distributed generation from renewable resources for residential applications.

I would like to express my gratitude to my supervisors, Florin Iov and Daniel-Ioan Stroe, for their support and valuable information provided during the development of the project.

Finally, I would like to thank my family and friends for being supportive during my study time at Aalborg University.

List of abbreviations

BESS	Battery energy storage system
CO_2	Carbon dioxide
PV	Photovoltaic
EMS	Energy management system
HEMS	Home energy management system
EIS	Electrochemical impedance spectroscopy
DP	Dual polarization
SOC	State of charge
OCV	Open-circuit voltage
EEC	Equivalent electrical circuit
HPPC	Hybrid pulse power characterization
PoC	Point of connection
WT	Wind turbine
GUI	Graphical user interface
MA	Moving average
MAF	Moving average functionality
Li-ion	Lithium-ion

Contents

Summary 3

Preface 4

List of abbreviations 5

1 Introduction 12

1.1 Background 15

1.2 Problem statement 19

1.3 Objectives 20

1.4 Scope and Limitations 20

1.5 Content of the report 21

2 State of the Art 23

2.1 Energy management system functionalities 23

2.2 Battery energy storage system models 23

2.2.1 Rint model 24

2.2.2 Thevenin model 25

2.2.3 DP model 25

3 System description 27

3.1 Battery energy storage system modeling 27

3.1.1 Battery performance parametrization 28

3.1.2 Battery modelling 37

3.1.3 Model validation 39

3.2 PV array performance model 41

3.3 Wind turbine performance model 42

4 Mission profile 43

4.1 Distributed generation power profiles 43

4.2 Demand profiles 44

5 Applications 47

5.1 Power smoothing 47
5.1.1 6 kW battery energy storage 48
5.1.2 3 kW battery energy storage 52
5.2 Energy blocks 56
5.2.1 6 kW battery energy storage 59
5.2.2 3 kW battery energy storage 61
6 Conclusion 65
7 Future work 67
Appendices 68
Appendix A: Short market overview of home energy management systems 68
Appendix B: Battery energy storage system 68
B1: Electrical parameters of the tested battery cell 68
B2: Capacity measurement values 69
B3: OCV measurement values 69
B4: EEC parameters 70
B5: The current profile applied to the battery during the verification of the performance model 71
Appendix C: Solar photovoltaic system 72
C1: Parameters of the solar PV 72
Appendix D: Wind turbine system 72
D1: Parameters of the wind turbine 72
Bibliography 73

LIST OF FIGURES

Figure 1-1 Installed solar photovoltaic capacity in Denmark for 2000-2016 [4] 12
Figure 1-2 Installed wind power capacity in Denmark for 2000-2016 [4] 13
Figure 1-3 Energy storage technologies and their applications [9] 14
Figure 1-4 Energy storage technologies efficiency with respect to the life time at 80% DOD [10] 14
Figure 1-5 Worldwide power consumption from renewable sources by sector in 2012 [12] 15
Figure 1-6 Adjustment of the residual load in Germany [7] 16
Figure 1-7 Total number of photovoltaic systems by capacity in Denmark in 2015 16
Figure 1-8 Total number of wind turbines by capacity in Denmark in February 2017 17
Figure 1-9 Subsidies for renewable energy in Denmark [16] 17
Figure 2-1 Schematic circuit of Rint model [31] 24
Figure 2-2 Schematic circuit of the Thevenin model [31] 25
Figure 2-3 Schematic circuit of the DP model [31] 26
Figure 3-1 Hybrid energy system architecture 27
Figure 3-2 Capacity measurement procedure 28
Figure 3-3 Voltage vs. Capacity during discharging of the battery cell, measured for all C-rates and T=25 degC 29
Figure 3-4 OCV measurement procedure 30
Figure 3-5 The OCV vs. SOC characteristic of the battery cell, measured at 25 degC . 31
Figure 3-6 The voltage response of the battery cell due to a discharging current pulse 32
Figure 3-7 Voltage response of the battery cell at discharge current pulses at various C-rates (SOC=50%, T=25 degC) 33
Figure 3-8 Internal resistance measurement procedure 33
Figure 3-9 Battery cell parameter extraction procedure 34
Figure 3-10 Ohmic resistance during pulse charging and discharging of the battery cell at different SOC values (T=25 degC, 1C-rate) 36
Figure 3-11 Polarization resistance during pulse charging and discharging of the battery cell at different SOC values (T=25 degC, 1C-rate) 36
Figure 3-12 Equivalent capacitance during pulse charging and discharging of the battery cell at different SOC values (T=25 degC, 1C-rate) 37
Figure 3-13 Equivalent circuit of the battery 37
Figure 3-14 Block diagram of the modeled battery cell used for validation 38

Figure 3-15 Current profile applied to the battery cell 39
Figure 3-16 Comparison between measured voltage and estimated voltage of the battery cell 40
Figure 3-17 Block diagram of the battery storage 41
Figure 3-18 Block diagram of the solar PV system 41
Figure 3-19 Block diagram of a simplified wind turbine 42
Figure 3-20 Power curve of the 10 kW wind turbine [41] 42
Figure 4-1 Input irradiance and PV power, during summer (left) and winter (right) 43
Figure 4-2 Input wind speed and WT power, during summer (left) and winter (right) 44
Figure 4-3 Household power consumption on a weekday, during summer (top) and during winter (bottom) 45
Figure 4-4 Household power consumption on a weekend day, during summer (top) and during winter (bottom) 46
Figure 5-1 Block diagram of the power smoothing functionality strategy 47
Figure 5-2 Simulation results of the first case (T=300 s, summer, 6 kW battery) 49
Figure 5-3 Comparison between the target power and grid power of the first case (T=300 s, summer, 6 kW battery) 49
Figure 5-4 Simulation results of the first case (T=300 s, winter, 6 kW battery) 50
Figure 5-5 Simulation results of the second case (T=900 s, summer, 6 kW battery) 51
Figure 5-6 Comparison between the target power and grid power of the second case (T=900 s, summer, 6 kW battery) 51
Figure 5-7 Simulation results of the second case (T=900 s, winter, 6 kW battery) 52
Figure 5-8 Simulation results of the first case (T=300 s, summer, 3 kW battery) 53
Figure 5-9 Comparison between the target power and grid power of the first case (T=300 s, summer, 3 kW battery) 53
Figure 5-10 Simulation results of the first case (T=300 s, winter, 3 kW battery) 54
Figure 5-11 Simulation results of the second case (T=900 s, summer, 3 kW battery) 54
Figure 5-12 Comparison between the target power and grid power of the second case (T=900 s, summer, 3 kW battery) 55
Figure 5-13 Simulation results of the second case (T=900 s, winter, 3 kW battery) 55
Figure 5-14 Overall power profile on a summer weekday 57
Figure 5-15 Overall power profile on a summer weekend 57
Figure 5-16 Overall power profile on a winter weekday 58
Figure 5-17 Overall power profile on a winter weekend 58
Figure 5-18 Battery power request on a summer weekday for a 6 kW battery 59
Figure 5-19 Battery power request on a summer weekend for a 6 kW battery 60

Figure 5-20 Battery power request on a winter weekday for a 6 kW battery 60
Figure 5-21 Battery power request on a winter weekend for a 6 kW battery 61
Figure 5-22 Battery power request on a summer weekday for a 3 kW battery 62
Figure 5-23 Battery power request on a summer weekend for a 3 kW battery 62
Figure 5-24 Battery power request on a winter weekday for a 3 kW battery 63
Figure 5-25 Battery power request on a winter weekend for a 3 kW battery 63
Figure 7-1 Internal resistance during pulse charging and discharging of the battery cell at different SOC values (T=25 degC, 1C-rate) 71
Figure 7-2 Steps of the applied current to the battery cell during the verification of the performance model 71

LIST OF TABLES

Table 1 Power smoothing deviations between the target power and the injected power 56
Table 2 Battery response for power smoothing application 56
Table 3 Battery response for power blocks application 64
Table 4 HEMS products- market overview [20] 68
Table 5 Electrical parameters of the tested battery cell 68
Table 6 Charging and discharging capacity measured for all C-rates 69
Table 7 OCV vs. SOC 69
Table 8 The EEC parameters for 0.1 C-rate 70
Table 9 Parameters of the solar PV in STC [44] 72
Table 10 Parameters of the wind turbine [41] 72

1 Introduction

Nowadays, more countries around the world are turning their consideration to renewable energy, as these technologies are continuously developing [1]. Also, renewable energy contribute at driving down the CO_2 emissions produced by fossil fuels, which increased significantly in concentration over the past century [2]. Renewable energy assured 23% of the total global generation in 2014 and it is predicted to hit 45% by 2030 [1].

Furthermore, the highlights of renewable energy are the installations of wind turbines and solar photovoltaics, which reached globally record levels in the last years. Solar photovoltaic is a promising future solution for energy production, with a rapidly improving technology and decreasing costs. It is estimated that solar PV will be able to cover 10%-30% of global energy demand between 2030 and 2050 [3].

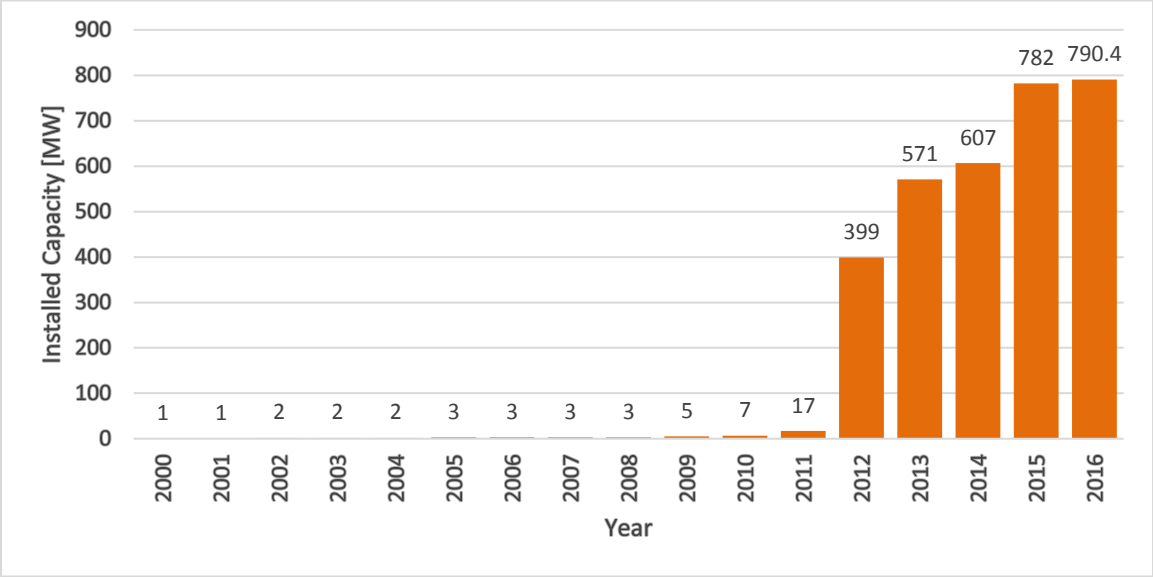

Figure 1-1 Installed solar photovoltaic capacity in Denmark for 2000-2016 [4]

Regarding Denmark, the solar photovoltaic total installed capacity has abruptly increased in the last years. According to IRENA (International Renewable Energy Agency), the solar photovoltaic installed capacity increased from 17 MW in 2011 to 399 MW in 2012 and continued to increase, reaching 790.4 MW in 2016 (Figure 1-1).

On the other hand, in the last 20 years, globally installed wind capacity increased 50 times, reaching 371 GW in 2014, with leaders like Denmark, China, USA or Germany [5].

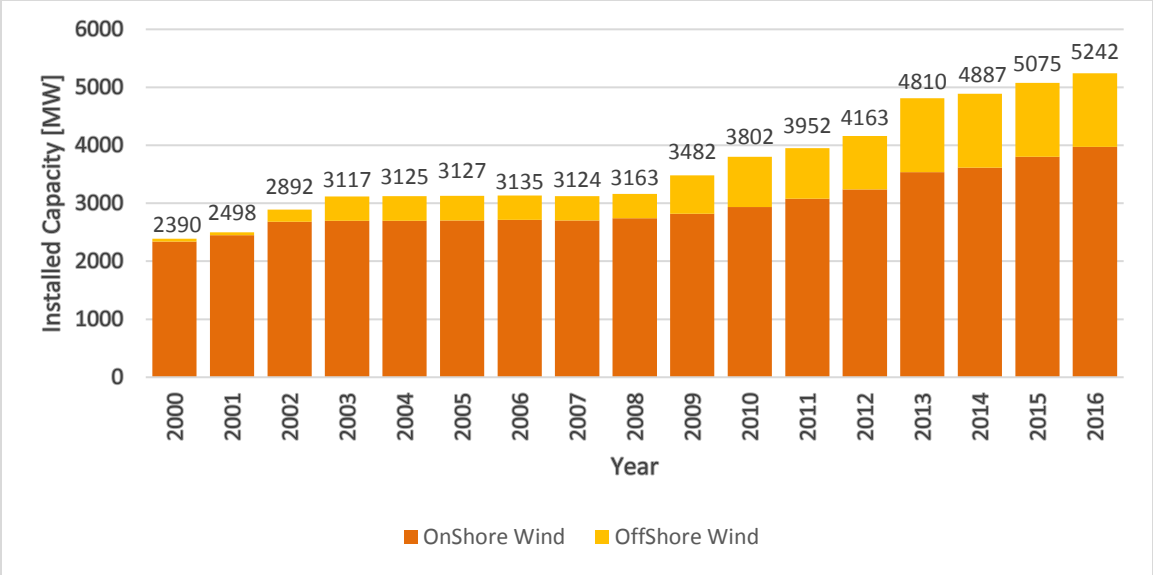

Figure 1-2 Installed wind power capacity in Denmark for 2000-2016 [4]

Denmark has always been a leader in power production sector from wind, reaching a total installed capacity from both onshore and offshore technology of 5242 MW in 2016 (Figure 1-2). According to the Danish Transmission System Operator, Energinet.dk, wind power represented 28.3% of the country's total electricity demand in 2011. Moreover, the current challenge for Denmark is to reach 50% of wind power penetration in 2020 [6]

Solar is presumed to became an important player in the energy field, by 2020 being expected to cover 8% of the total European power demand. Aggregated with wind generation, it will require a more flexible system. Hence, new forms of system stability will be needed to assure a better use of the electricity when power is cheap and to sustain the grid during peak hours. In order to achieve this, storage systems could be used to respond to the balancing needs, by storing the excess power from renewables and releasing it when the production is low [7].

Renewable energy capabilities and the new policies regarding the electricity field modernization are supporting the battery energy storage systems implementation. From a technological point of view, battery storage is advanced and very accessible. Nevertheless, some disadvantages regarding the performance and safety issues, regulatory approvals or utility allowance still must be taken into consideration [8].

In the power sector, battery storage can be engaged in various way, providing multiple services (i.e. transmission congestion relief, voltage support, power quality and reliability,

electric energy time-shift), covering transmission and distribution sector or customer energy management services [8]

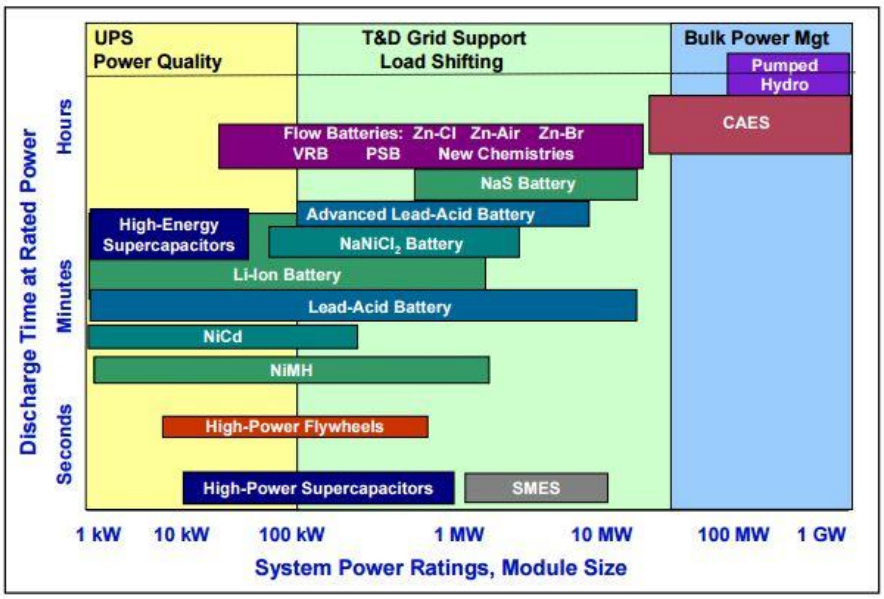

Figure 1-3 Energy storage technologies and their applications [9]

Figure 1-3 illustrates the maturity and arising storage technologies organized in categories of power quality, grid support and power management.

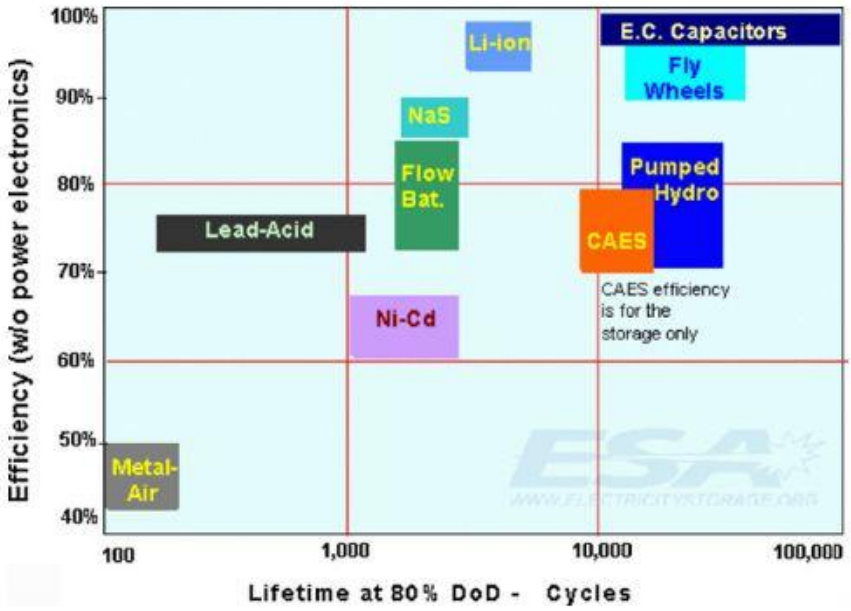

Figure 1-4 Energy storage technologies efficiency with respect to the life time at 80% DOD [10]

Compared to other batteries, Lithium-Ion batteries have high efficiency, high energy and power density, more stable charging and discharging characteristics and can manage deep discharges with small impacts on lifetime. These technologies continue to improve, which make them popular in the power sector [11].

1.1 Background

The utilization of renewable sources can be found in various worldwide fields. As it can be seen in Figure 1-5, 50.4% of consumption from renewables is used in residential, commercial and public areas. Along with the fast development of technology in sustainable energy field and the increase of energy demand, the usage of renewable energy has gained a big interest for smart households [12].

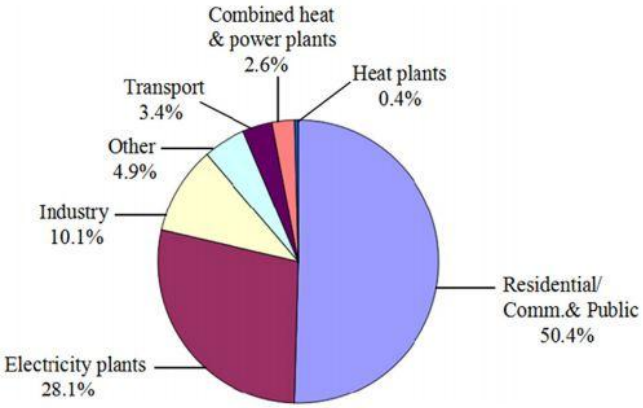

Figure 1-5 Worldwide power consumption from renewable sources by sector in 2012 [12]

Figure 1-6 emphasizes how solar and wind power could reduce the need for residual load (the difference between energy demand and energy production), in Germany, starting with 2020. Solar power is able to reduce the residual load during the day, while wind power could reduce it during the evening, when power demand is high. Energy storage could be an optimal solution to store excess energy during off-peak hours and release it during peak-hours, when the utility power price is high [7].

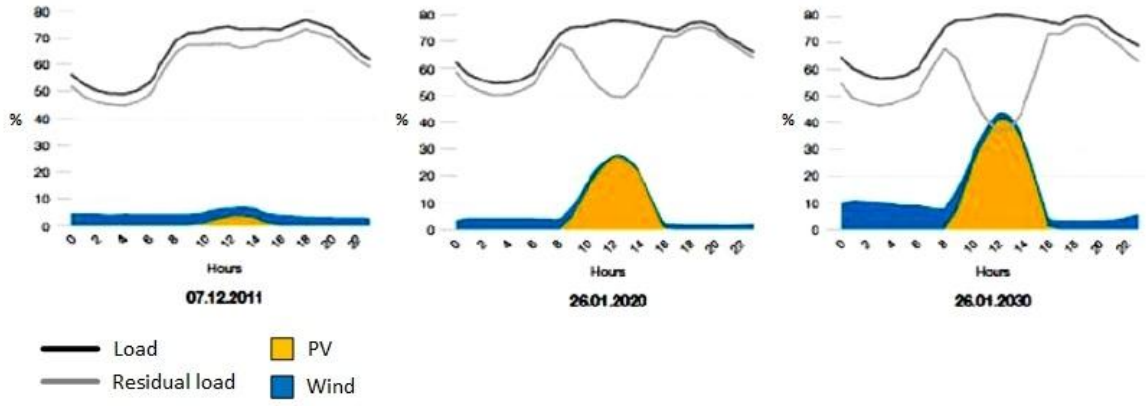

Figure 1-6 Adjustment of the residual load in Germany [7]

In Denmark, municipalities started to play a more active role in the deployment of PV systems in the country. A Danish PV association called Dansk Solcelle Forening, formulated a scheme which aims that by 2020, 5% of the electricity from the private households coming from photovoltaics. The future PV market growth in Denmark depends on the impact of the net-metering scheme. In 2013, new regulations took place regarding PV installations. They were set to 60 øre/kWh for the first 10 years and 40 øre/kWh for the following 10 years. However, the number of PV installations not applying for net-metering scheme, but operating for self-consumption are growing [13].

Figure 1-7 illustrates the total number of Danish photovoltaic systems in 2015, according to Energinet.dk. At the end of 2015, a subsidy scheme aimed at large photovoltaic plants (400 kW), therefore a big number of large photovoltaic plants were installed in this period. This amount of photovoltaics will be seen when the data will be updated with information regarding year 2016 [14].

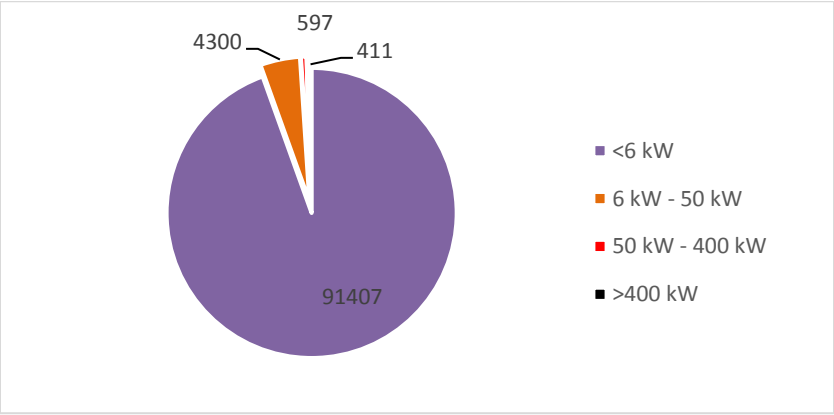

Figure 1-7 Total number of photovoltaic systems by capacity in Denmark in 2015

For small wind turbines, Energinet.dk offers subsidies for 12 years from the grid connection, and this is set for 212 øre/kWh for wind turbines smaller than 10 kW and 132 øre/kWh for wind turbines between 10 kW- 25 kW [14].

In Figure 1-8 it can be seen the total numbers of currently (February 2017) working wind turbines in Denmark, according to Danish Energy Agency [15].

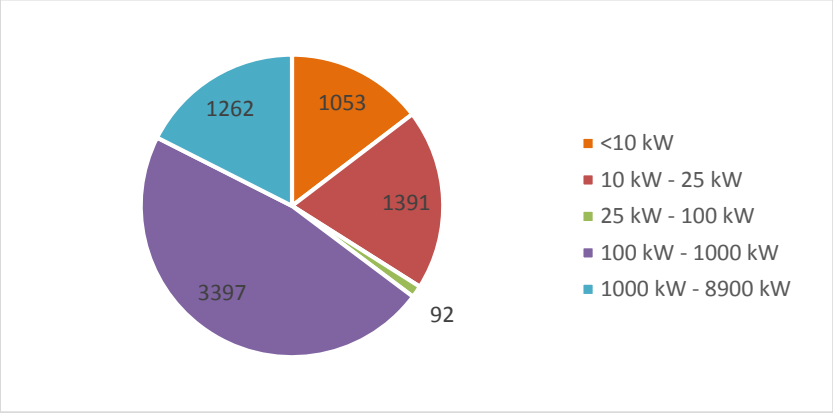

Figure 1-8 Total number of wind turbines by capacity in Denmark in February 2017

Figure 1-9 shows that subsidies offered for renewable energy in Denmark are in a continuous ascension, reaching almost 8 billion DKK in 2015 [16].

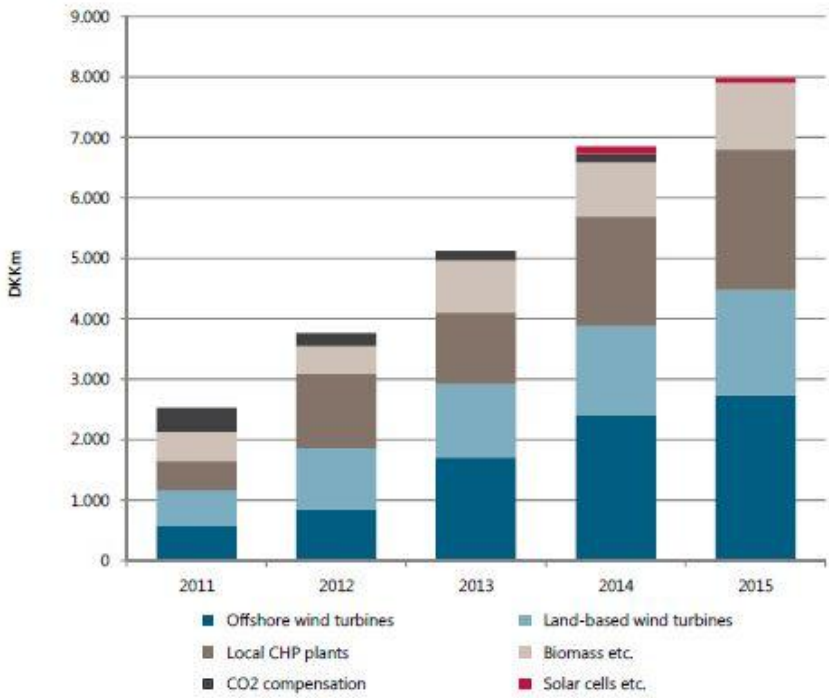

Figure 1-9 Subsidies for renewable energy in Denmark [16]

For wind turbines, subsidies constituting 4.5 billion DKK have been paid in 2015 and 74 million DKK for solar cells [16].

A satisfaction survey regarding the payment of the subsidies has been conducted among 90 000 solar cells customers, and concluded that 65% of them responded positive towards Energinet.dk's administration. The aim for Energinet.dk is to achieve 80% satisfaction level in 2017 [16].

Furthermore, for a better planning of the response, there are energy management systems (EMS) that evaluate the energy prices and other external factors without the customer intervention. The EMS is a tool that can evaluate and improve the energy generation-consumption profile according to electricity prices and customer requests. It communicates with household appliances and the utility grid and receive information regarding the solar/wind power generation and electricity prices to improve the overall energy efficiency by adjusting and scheduling the production/consumption [17].

It has been proved that a home energy management system (HEMS) could reduce the operating cost of electricity or reduce the household energy peak demand. For instance, in [18] it has been concluded that the integration of EMS could reduce the electricity cost by 20% and reduce the peak demand by 50%.

The HEMS market has been considerably expanded due to the interest of consumers in home automation devices. Additionally, residential renewables, electric vehicles and smart appliances have also an impact on HEMS market expansion [19]. An overview of HEMS products can be found in Table 4, Appendix A, containing some of the most important suppliers on the market [20].

HEMS market is very wide, including many companies that provide various products for home energy management. These products comprise smart appliances, in-home displays, smart lighting/hubs/switches, smart thermostats etc. These products are easily controllable, provide information to customer and manage the energy usage. The main drawback of these technologies could be the price, which is high compared to normal products of the same category.

Further, regarding the utility side, a distribution energy management system allows short-term energy scheduling at minimum costs based on power production and demand. Moreover, it uses various methods to forecast the power generation from renewable sources and to optimize the generation from power plants. It could also predict the power

demand of non-schedulable loads and optimize the power demand of controllable loads at the required system reliability [17].

1.2 Problem statement

Currently, a new challenge is growing in the energy power systems field, which is the increase of distributed generation from renewable sources. The main drawback is the intermittency in power generation from these sources, thus new systems are needed to satisfy the continuously growth of energy demand. Frequently, for a better use of the variable power production from renewable energy, these systems are integrated with energy storage (especially for off-grid applications) [18].

The storage systems associated with photovoltaic and wind energy are a promising solution for future households, in maximizing the residential self-consumption, reducing the grid costs, power-smoothing, peak-shaving. The system could be viable in areas with high solar/wind penetration level and high retail electricity prices or areas where there is no access to the power grid [21].

The power variations in PV generation emerge when instantaneous passage of clouds cover the solar arrays. The PV output is difficult to be predicted, due to the PV performance being reliant on cloud shadowing, solar irradiance, temperature, wind etc [22].

Unlike solar power, where the power is generated only during the day, due to the presence of the sun, the wind turbine can produce power also during the night. Therefore, in some regions or during some periods of the year, the peak output from wind could be in the night when the demand is low [23].

The power produced by the wind turbine and PV system is dependent on weather conditions, hence even slight changes in wind speed or sunlight can cause power fluctuations in the system. To attenuate this problem, the power sources can be integrated with storage systems. Hence, a better usage of the produced power could be gained, by balancing the demand with the production or attenuating the fluctuations produced by the generation [24].

1.3 Objectives

Optimum utilization of the hybrid renewable energy and the quality of the power injected into the grid, simultaneously with the proper use of the storage system, are essential for a reliable operation and minimum costs.

The main goal of the project is to develop optimum power and energy management strategies for a household application, considering the integration of wind power and photovoltaics together with battery energy storage system.

The research challenge is to accurately model a battery storage system, which can provide suitable support for the studied applications.

Furthermore, the first objective of the study is to implement a power smoothing functionality by using the battery, to smoothen the power fluctuations induced by renewable sources, i.e. wind and solar photovoltaics, for a better quality of the power before being injected to the utility grid.

The second objective is to minimize the energy exchange with the utility grid and hence to minimize the energy bill by coordinated energy management of the energy storage system considering generation and consumption profiles.

To exploit the power from the renewable sources to the maximum and to meet the house demand, the battery must be capable to minimize the energy bill. This can be done by storing the energy during off-peak hours, when the price is low and release it during peak-hours, when the price is high.

1.4 Scope and Limitations

- The main scope of the project is to develop an optimum energy management system of the wind/PV and battery energy storage, in order to obtain the most favorable operation or use.
- To maximize the power consumption from renewable sources and to minimize the electricity cost, the battery storage is an important key of the overall system. Therefore, the research challenge is to develop a performance model of the battery dedicated to integration studies, based on laboratory measurements.
- The system performance will be tested and verified by simulation using real load demand profiles and weather data (solar irradiation and wind speed) for different periods of the week and year.

- The performance models of the wind turbine and PV system will be studied, without considering power converter topology, internal control loops, type of grid, i.e. AC or DC, or other devices, therefore the type of the current does not have a relevance in this study.
- Moreover, only the active power on the generation/storage/consumption side will be studied, a fixed voltage being considered, the DC link voltage, i.e. 600 V.
- The electrical connections are neglected.
- The power grid characteristics will not be studied and modeled. The main concern is the power exchange in the PoC (point of connection) with the grid.
- Two sizes of the battery will be considered based on typical commercial offers, and the results will be compared and analyzed.
- Sizing of energy storage for considered applications is out of scope.
- Simultaneously allocation of services and sharing is out of scope.

1.5 Content of the report

The project is organized in 5 chapters, each including several subchapters.

Chapter 1 introduces an overview of the renewable energy, particularly solar PV and wind power sources. Further, the background material of the energy management systems is presented, comprising the status and an overview of the EMS market. Moreover, a summary of the Danish solar and wind systems is presented. In addition to the background, the first chapter includes the problem statement, research objectives, scope and limitations and the outline of the work.

Chapter 2 presents the state of the art regarding the energy management system and an overview of the Danish electricity market. Also, the most commonly used battery electrical circuits are presented.

In Chapter 3 the architecture of the system is described and the performance models for the generation side, the photovoltaic system and the wind turbine. Furthermore, the parametrization of the battery has been performed in order to better understand the dynamics, followed by a model implemented in a simulation tool.

Chapter 4 comprises an overview of the distributed generation power profiles and demand power profiles, that will be used in the simulations.

Chapter 5 describes the applications that have been proposed and the results of the simulations for each of the battery and for every case and period considered.

Finally, in chapter 6, conclusions are presented together with ideas for future work regarding the current study.

2 State of the Art

2.1 Energy management system functionalities

The performance of the hybrid distributed generation depends on the power and energy management strategy. Together with the battery storage system, renewable sources could improve the overall system efficiency and dynamic response. A power management strategy could be decisive for balancing between the efficiency and the system performance [25].

In the current paper, the power management determines the suitable power level to be generated while satisfying the power demand and storing sufficient energy in the battery energy storage. If there is not enough available power from renewable resources or battery storage, the system relies on the power grid. Reciprocally, if the power fulfills all the needs, it could be sell to the utility grid.

As mentioned previously, the energy management method proposed in this study consists of planning the charging/discharging of the battery with regard to the typical power pattern of the house. The power pattern is based on the power generation from RE sources and power demand.

2.2 Battery energy storage system models

Different battery modeling approaches have been developed in order to estimate the battery performance. There are three general categories that comprise the existing battery models: electrochemical modeling, mathematical and electrical [26].

The most accurate battery model is the electrochemical model, which uses non-linear differential equations to describe the chemical processes inside the cells in a very detailed manner [27].

Mathematical models have a reduced accuracy, due to several assumptions, and reduced complexity too. The parametrization is based on the battery data-sheet and therefore, these models are used only for some applications and the errors could reach 5%-20% [26]

Electrical models are used to predict the static and dynamic behavior (mainly the terminal output voltage) of a real-life battery under different operating conditions [28]. They are equivalent electrical models which use simple circuit elements (voltage sources, resistors

and capacitors), having an accuracy between the two models presented previously (1%-5% error). The parametrization is based on laboratory tests and it has a medium computation complexity. Hence, this approach is easy to handle, simple, with a good accuracy and very intuitive for electrical engineers [26].

To parametrize an electrical battery model, two methods can be used: the dc-pulse method and the EIS method. The dc-pulse technique consists of measurement of the battery's voltage after a dc-pulse has been applied and subsequently determines the battery resistance, and the second method uses the EIS technique to obtain an equivalent electrical circuit [29].

The most commonly used equivalent circuit models in battery studies are the Rint model, the Thevenin model ant the DP model [30]. In the following section, these approaches will be briefly introduced.

2.2.1 Rint model

Figure 2-1 illustrates the schematic diagram of a Rint model, described by equation (1). The circuit is composed of a voltage source U_{oc}, which represents the open circuit voltage of the battery and a resistance R_0, which are used to predict the voltage at the battery terminals U_L. The open circuit voltage and the resistance are dependent of state-of-charge (SOC) and temperature [31].

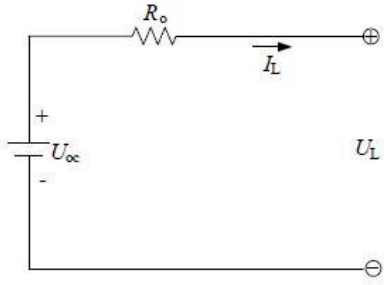

Figure 2-1 Schematic circuit of Rint model [31]

$$U_L = U_{oc} - I_L R_0 \quad (1)$$

However, the model is applicable for some circuit simulations, where many assumptions have to be made and where SOC is not considered important [32]. Therefore, this model is not suitable for this study.

2.2.2 Thevenin model

The Thevenin circuit is composed mainly of three parts including a SOC dependent voltage source U_{oc} (open-circuit voltage), in series with the ohmic resistance R_0 and a single RC circuit. The RC network is composed of a polarization resistance R_{Th} and an equivalent capacitance C_{Th} (Figure 2-2).

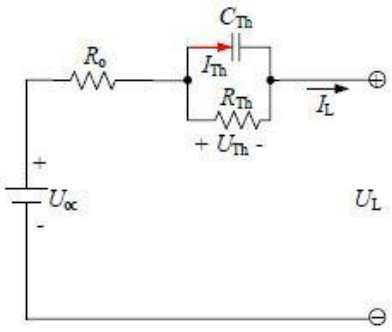

Figure 2-2 Schematic circuit of the Thevenin model [31]

$$\dot{U}_{Th} = -\frac{U_{Th}}{R_{Th}C_{Th}} + \frac{I_L}{C_{Th}} \tag{2}$$

$$U_L = U_{oc} - U_{Th} - I_L R_o \tag{3}$$

The model is more accurate than the previous example, but the tests showed that the difference between concentration polarization and electrochemical polarization results to imprecise simulation at the end of charge/discharge [31]. Nevertheless, Thevenin model is satisfactory for the purpose of this study.

2.2.3 DP model

Thevenin model has derivative models (dual polarization model) which are improved structures, with additional components (RC parallel networks) added to increase the accuracy. The circuit illustrated in Figure 2-3, is composed of an open-circuit voltage U_{oc}, the ohmic resistance R_0, and two RC branches representing the polarization resistances. R_{pa} is the resistance which characterizes the electrochemical polarization and R_{pc} is the resistance which characterizes the concentration polarization. The capacitances C_{pa} and C_{pc} are used to characterize the transient response of the battery during charging/discharging and to depict the two polarizations separately. Unlike Thevenin model, DP model allows to simulate the concentration polarization and the electrochemical polarization independently. The disadvantage of this solution is the

additional mathematical equations and the increased computing time, which make it unsuitable for the current study [26].

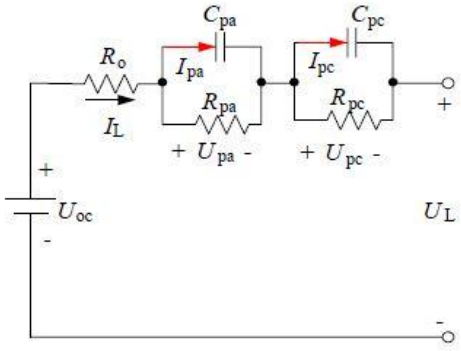

Figure 2-3 Schematic circuit of the DP model [31]

$$\dot{U}_{pa} = -\frac{U_{pa}}{R_{pa}C_{pa}} + \frac{I_L}{C_{pa}} \tag{4}$$

$$\dot{U}_{pc} = -\frac{U_{pc}}{R_{pc}C_{pc}} + \frac{I_L}{C_{pc}} \tag{5}$$

$$U_L = U_{oc} - U_{pa} - U_{pc} - I_L R_o \tag{6}$$

After conducting different methods and algorithms of parameters identification for every electrical model presented previously, [31] concluded that the Thevenin model and its derivative, DP model have better dynamic simulation outcomes, being an optimal solution for modeling lithium-ion batteries.

In this work, the Thevenin circuit has been chosen to model the battery dynamic behavior, using the dc-pulse method for parametrization of the circuit.

3 System description

Figure 3-1 illustrates the main architecture of the residential hybrid energy system with battery storage. The system is composed of 17 PV modules with a rated power of 360 W each (approximately 6 kW), a 10 kW wind turbine and a Lithium-Ion battery energy storage system. The smart meter between the household side and the utility side, permits the power exchange with the public grid.

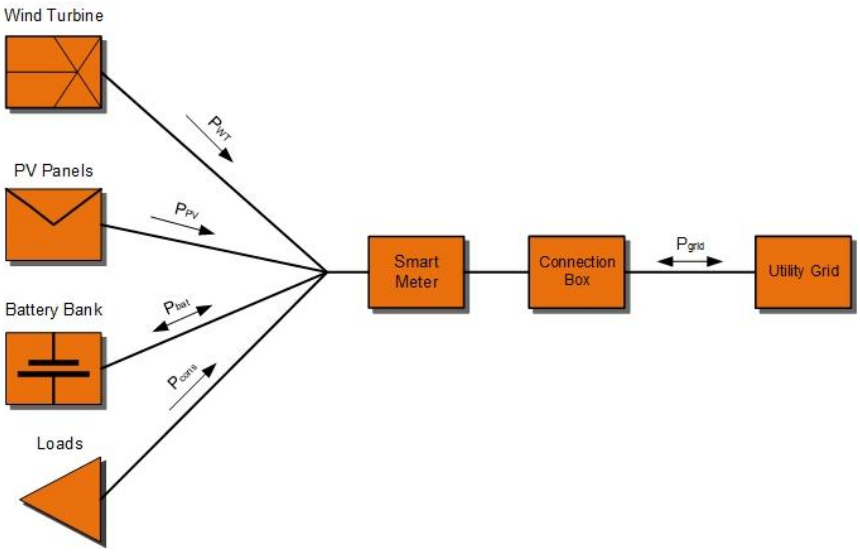

Figure 3-1 Hybrid energy system architecture

In the next subsections, the performance of every component of the residential hybrid energy system will be presented.

3.1 Battery energy storage system modeling

In this project, the Lithium-ion battery technology was considered for modeling. A performance model has been developed to better understand the behavior of the battery in different operating conditions (state of charge, load current). The electrical equivalent circuit proposed in order to study the dynamic performance of the battery is the Thevenin model presented earlier (Figure 2-2). To parametrize the performance model, laboratory experiments have been performed for measuring the battery capacity, open-circuit voltage and internal resistance. After the parametrization is completed, the model of the battery will be implemented in a simulation tool according to the measured parameters. The electrical parameters of the tested battery cell can be found in Table 5, Appendix B.

All the experiments have been conducted on a 2.5 Ah battery cell. The nominal voltage of the battery is 3.3 V, as it can be seen in Table 5. However, this value corresponds to 50% SOC, therefore in the current study a voltage range between 3 V and 3.6 V will be considered.

3.1.1 Battery performance parametrization

To investigate and model the battery, it has been subjected to several tests: capacity measurement, open-circuit voltage measurement and internal resistance measurement, under different current rates (C-rates) and a constant temperature.

A. Capacity measurement

To investigate the performance and capability of a battery, a capacity measurement test is needed. Considering that the capacity depends mostly on the temperature and the current, the test has to be carried for different current rates [33].

In this project, the temperature has been considered constant (i.e. 25 °C) and five different C-rates have been used (i.e. C/2, 1C, 2C, 3C and 4C). The capacity measurement follows the procedure presented in Figure 3-2, and the measured values for both charging and discharging experiment are shown in Table 6, Appendix B.

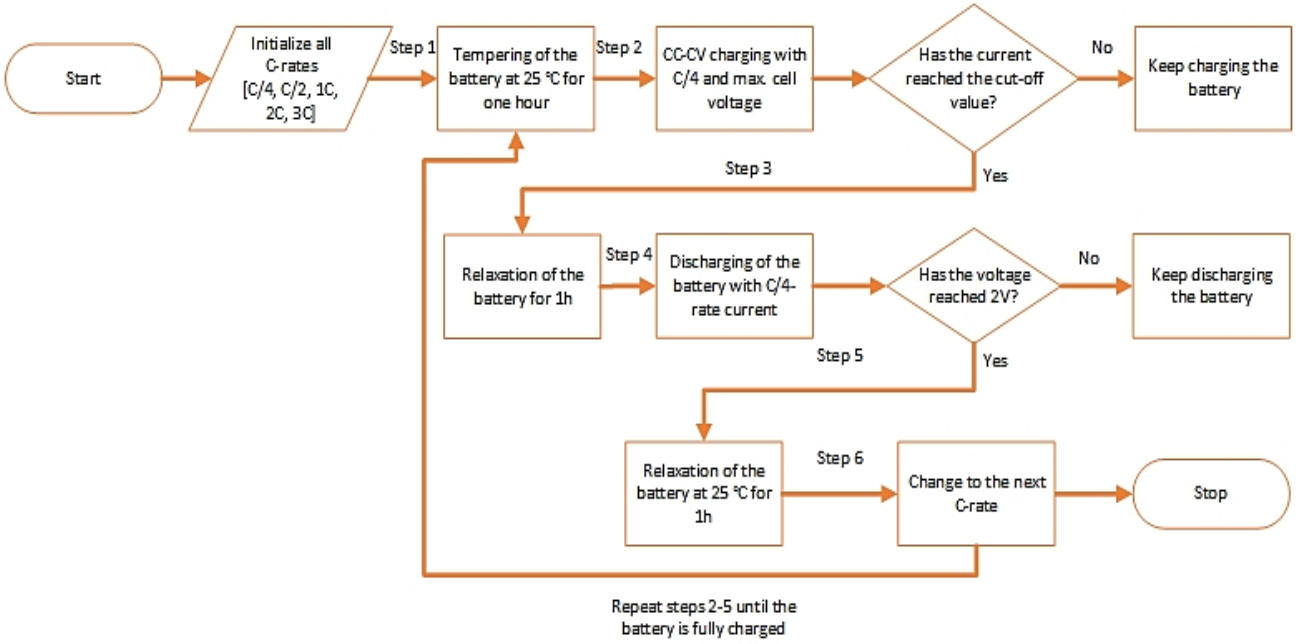

Figure 3-2 Capacity measurement procedure

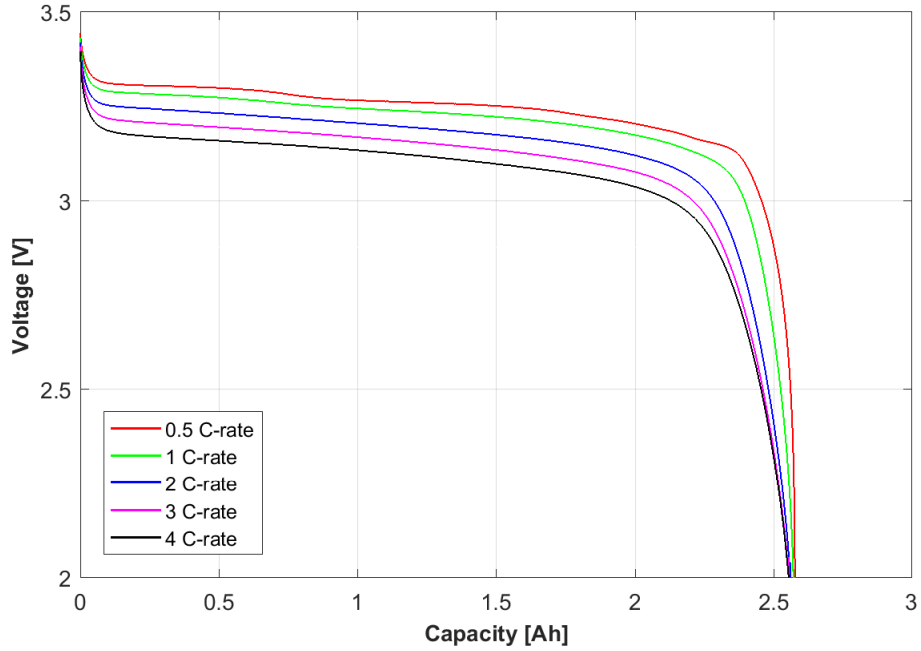

Figure 3-3 Voltage vs. Capacity during discharging of the battery cell, measured for all C-rates and T=25 degC

B. OCV measurement

Open-circuit voltage is an important parameter to be considered when building a battery model. The open-circuit voltage is also dependent on the operation conditions of the battery (i.e. SOC, temperature). Another aspect that should be taken into consideration during the OCV vs. SOC test is the relaxation time. It has been observed that the OCV depends on it during the relaxation test, hence the longer the rest time, the more precise the OCV measurement is [34].

The goal of this test is to determine the OCV vs. SOC characteristic of the battery at a temperature of 25 °C. This characteristic will be used in building the performance model of the battery, therefore an accurate measurement is important.

The procedure for measuring the battery's OCV characteristic is presented in Figure 3-4.

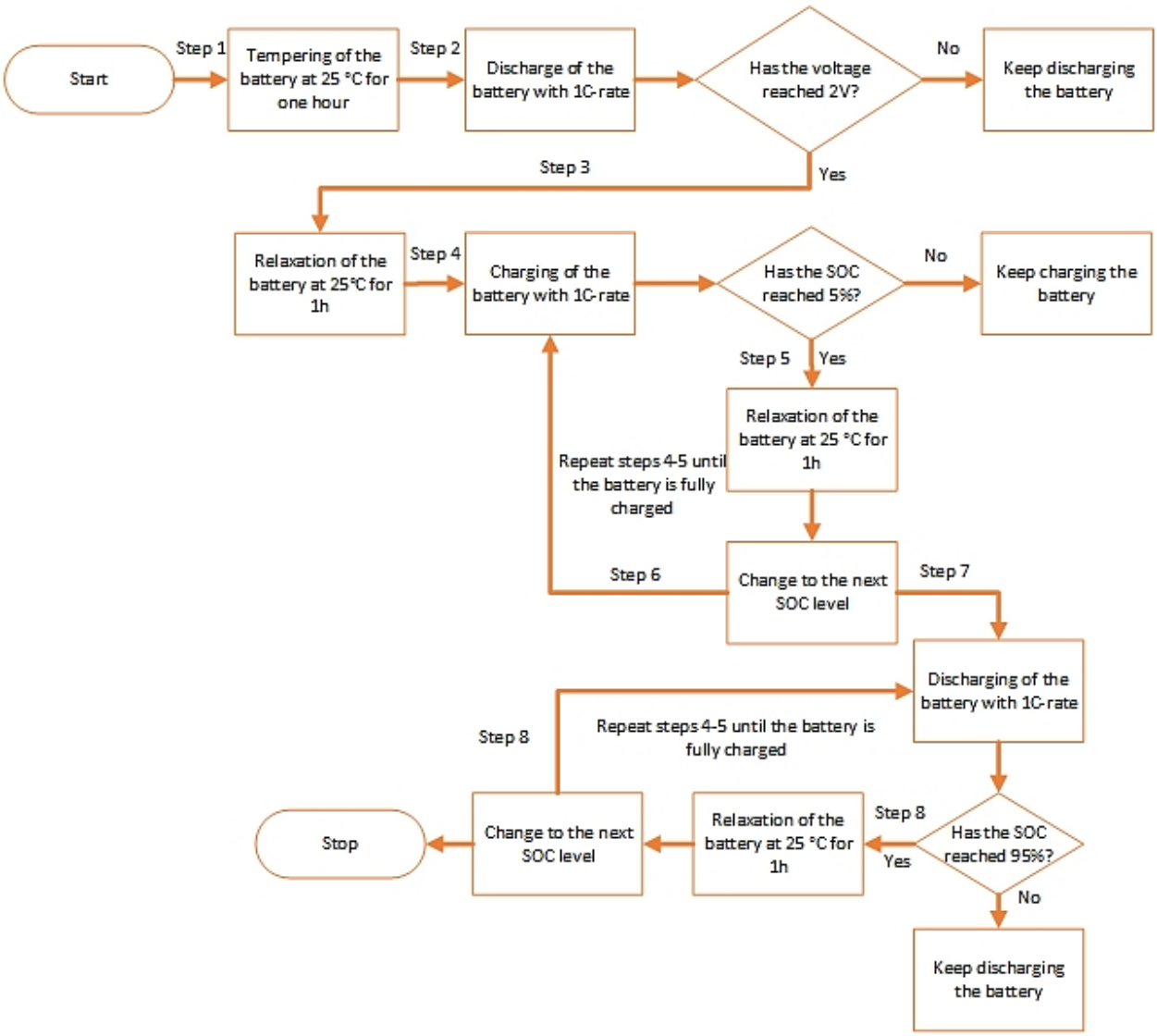

Figure 3-4 OCV measurement procedure

The OCV vs. SOC characteristic of the battery cell, measured at 25 °C, for both charging and discharging cases is depicted in Figure 3-5.

The extracted OCV values for both charging and discharging experiment, for every level of SOC are given in Table 7, Appendix B.

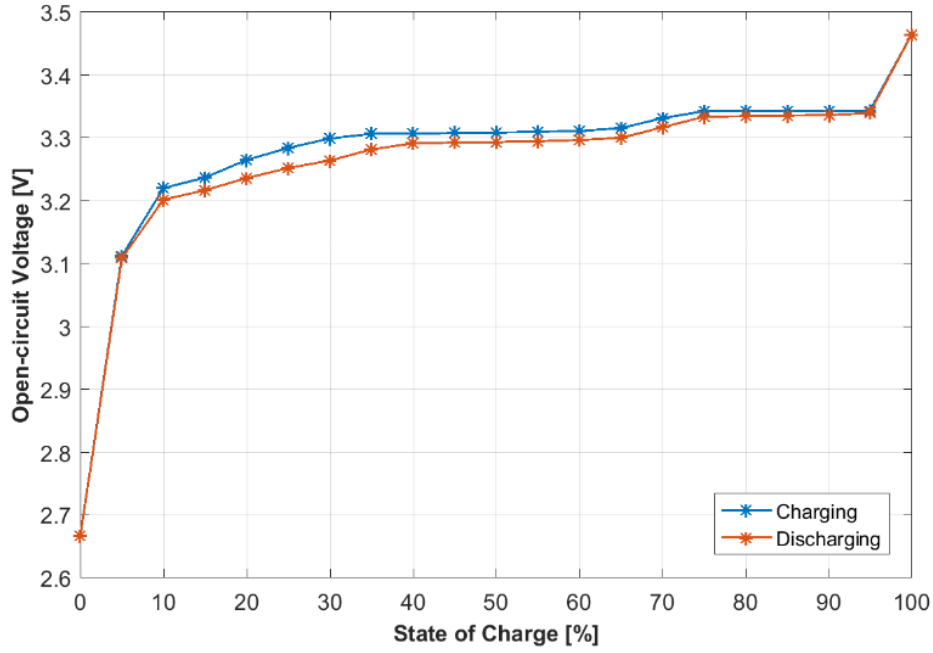

Figure 3-5 The OCV vs. SOC characteristic of the battery cell, measured at 25 degC

C. Internal resistance measurement

The internal resistance measurement is an important test, because it gives information about the battery dynamic behavior.

In order to determine the EEC parameters of the model, a hybrid pulse power characterization (HPPC) method has been followed. The internal resistance of the battery was determined by applying charging and discharging current pulses for the entire SOC interval with 5% SOC resolution (i.e. 5%-95% SOC), with different C-rates (i.e. C/10, C/2, 1C, 2C, 3C, 4C). The test applied to the battery cell comprises consecutive charging and discharging pulses with a duration of 18 seconds and a relaxation time between pulses of 15 minutes.

Figure 3-6 illustrates the voltage response of the battery cell caused by a discharging current pulse.

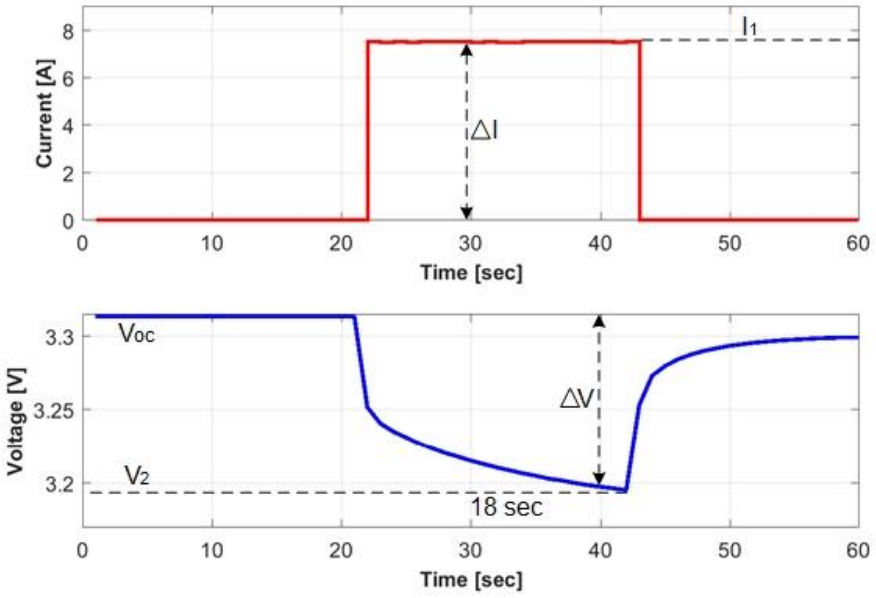

Figure 3-6 The voltage response of the battery cell due to a discharging current pulse

The internal resistance of the battery is computed based on Ohm's Law [35]:

$$R_i = \frac{\Delta V}{\Delta I} = \frac{V_2 - V_{OC}}{I_1} \tag{7}$$

Where:

R_i is the internal resistance of the battery, measured in [Ω]; ΔV is the change in the voltage caused by the discharging pulse, measured in [V]; ΔI is the change in the current caused by the discharging pulse, measured in [A]; V_1 is the voltage measured after 18 seconds, measured in [V]; V_0 is the initial voltage, measured before applying the discharging pulse, measured in [V]; I_1 is the measured current pulse, measured in [A]. All these parameters are described by Figure 3-6.

Figure 3-7 exemplifies the voltage response of the battery cell to current pulses, of various C-rates, at 50 % SOC and 25 °C. Similar behavior of the voltage has been observed for the other SOC levels.

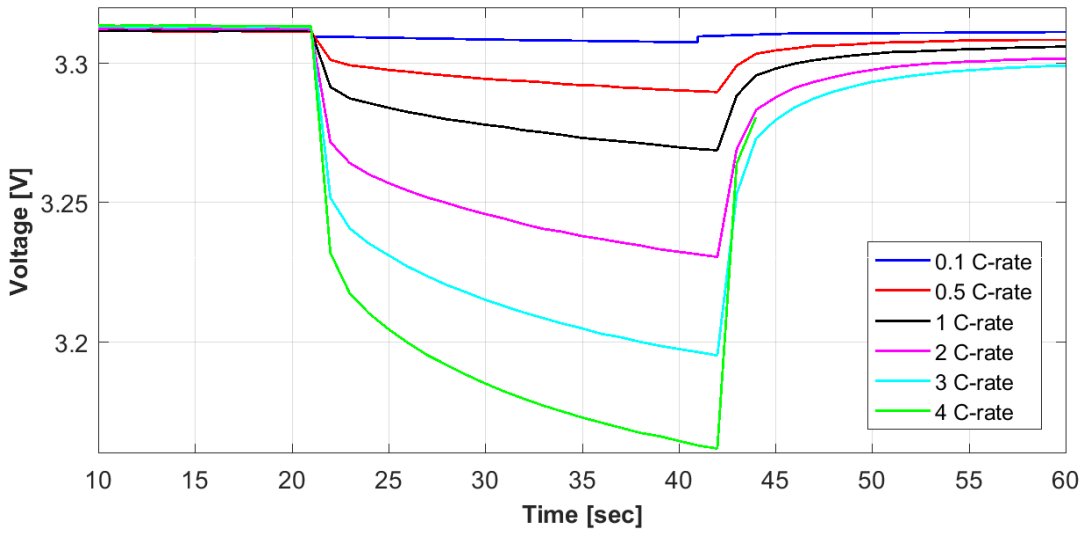

Figure 3-7 Voltage response of the battery cell at discharge current pulses at various C-rates (SOC=50%, T=25 degC)

The components of the EEC (R_0, R_{Th}, C_{Th}) are calculated, based on the battery's voltage response.

The experimental method implemented in the laboratory, for measuring the internal resistance, follows the steps presented in Figure 3-8.

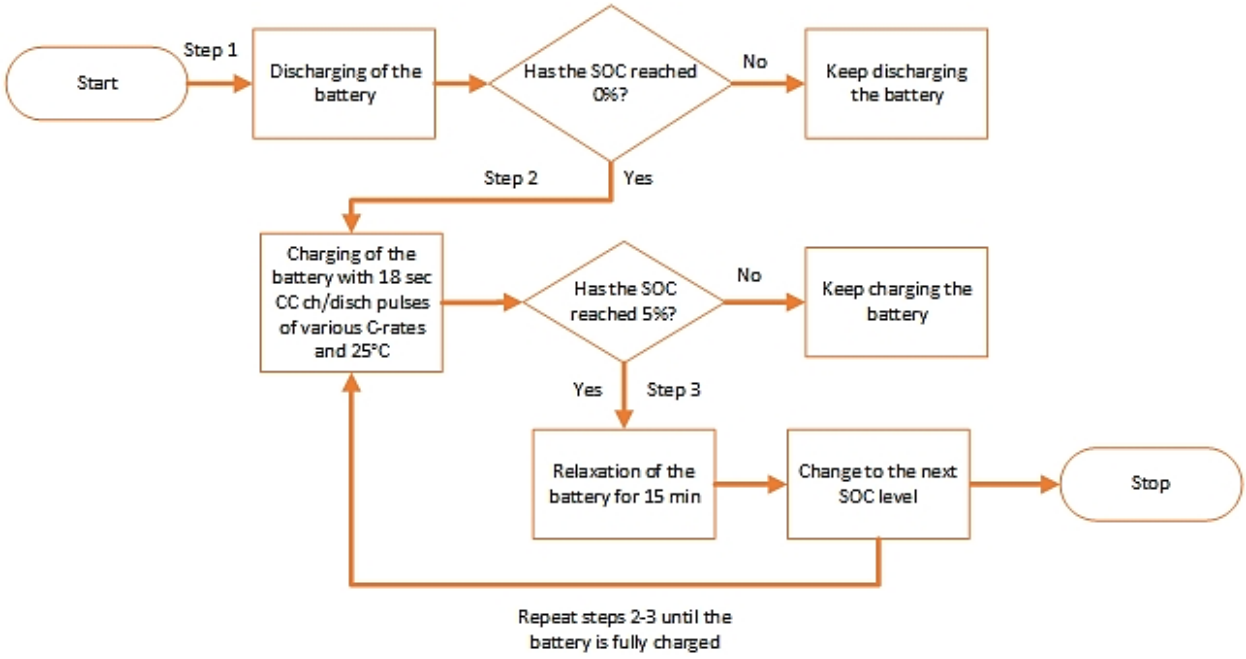

Figure 3-8 Internal resistance measurement procedure

Figure 3-9 illustrates the voltage positions on the voltage response curve, used for EEC parameters calculation, which is described in the following paragraphs.

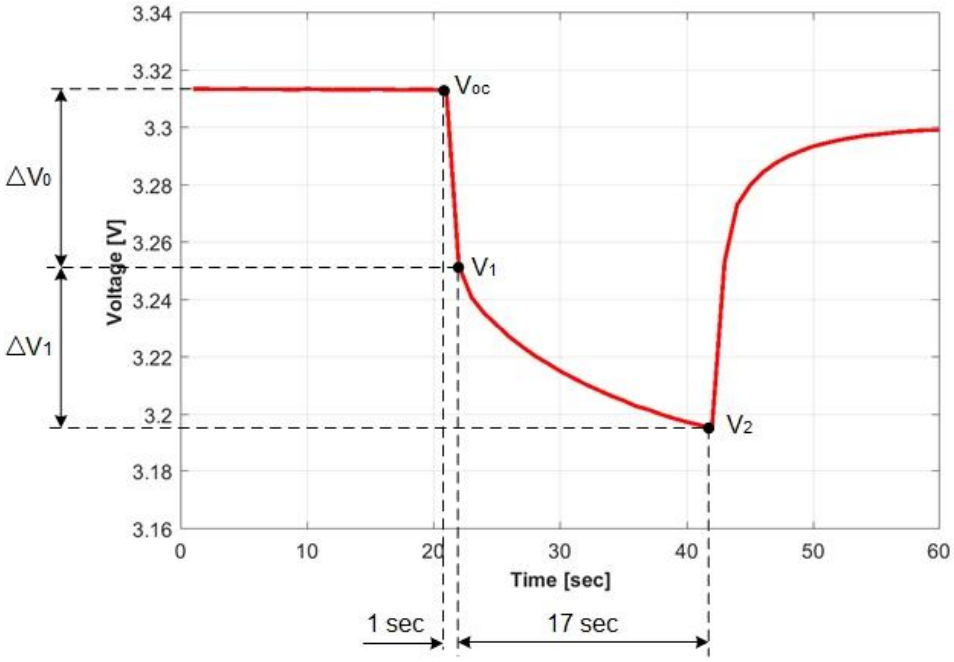

Figure 3-9 Battery cell parameter extraction procedure

The ohmic resistance R_0 can be calculated following the equation below [36]:

$$R_0 = \frac{V_{OC} - V_1}{I} \tag{8}$$

Where:

R_0 is the ohmic resistance of the battery, measured in [Ω]; V_{OC} is the voltage at the end of the 15-minute relaxation, measured in [V]; V_1 is the voltage after 1 second after the current pulse ends, measured in [V] and I is the amplitude of the current pulse, measured in [A].

Furthermore, the polarization resistance R_{Th} (due to charge transfer and diffusion process) is calculated with [36]:

$$R_{Th} = \frac{V_1 - V_2}{I} \tag{9}$$

Where:

R_{Th} is the polarization resistance of the battery, measured in [Ω]; V_1 is the voltage after 1 second after the current pulse is applied, measured in [V]: V_2 is the voltage after 18 seconds after the current pulse is applied, measured in [V] and I is the amplitude of the current pulse, measured in [A].

Finally, the capacitance C_{Th} can be calculated by knowing the time constant τ of the RC element [36]:

$$\tau = \frac{t}{\ln\left(\frac{V_2}{V_1}\right)} \tag{10}$$

Where:

τ is the time constant of the RC element, measured in [sec]; t is the time between V_2 and V_1, t=17 [sec].

Therefore, the capacitance is calculated [36]:

$$C_{Th} = \frac{\tau}{R_{Th}} \tag{11}$$

An example of the calculated EEC parameters for both charging and discharging case for 0.1 C-rate are shown in Table 8, Appendix B.

Figure 3-10, Figure 3-11 and Figure 3-12 emphasize the ohmic and polarization resistances and the equivalent capacitance of the battery cell, measured for both charging and discharging case, measured at 25 °C and different SOC levels.

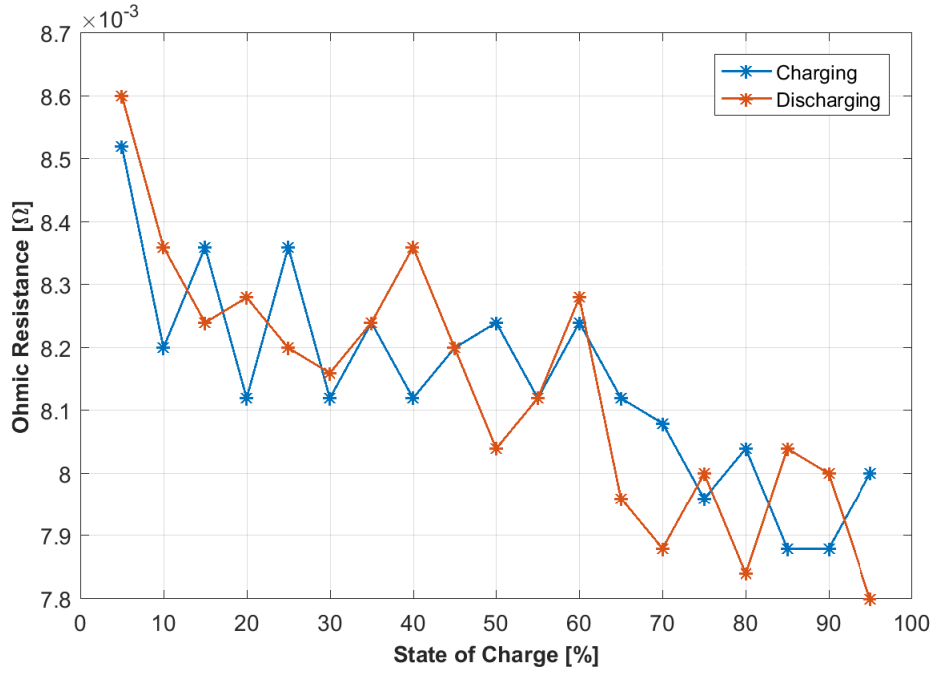

Figure 3-10 Ohmic resistance during pulse charging and discharging of the battery cell at different SOC values (T=25 degC, 1C-rate)

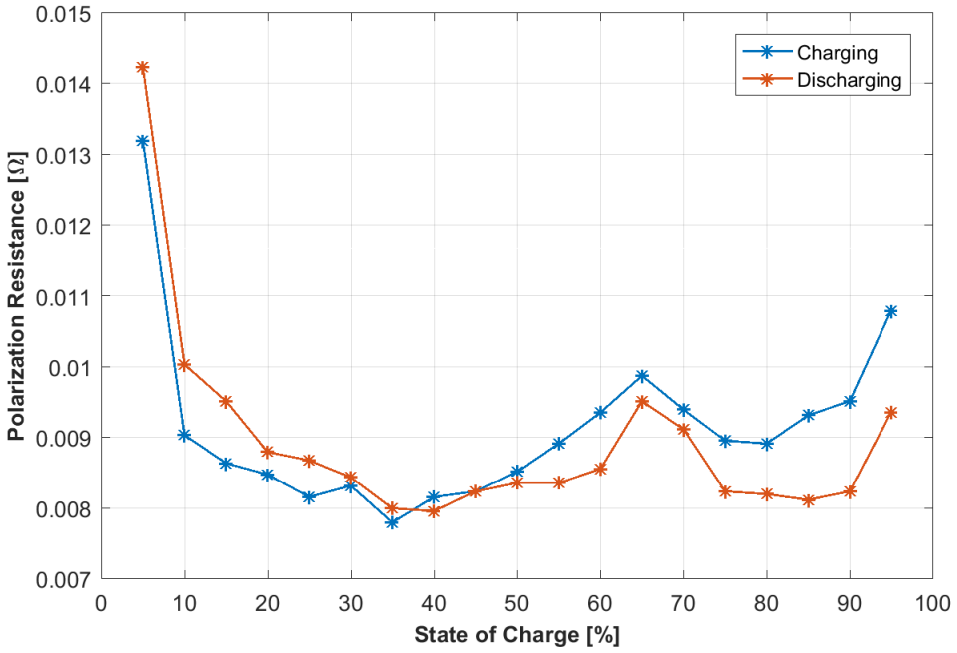

Figure 3-11 Polarization resistance during pulse charging and discharging of the battery cell at different SOC values (T=25 degC, 1C-rate)

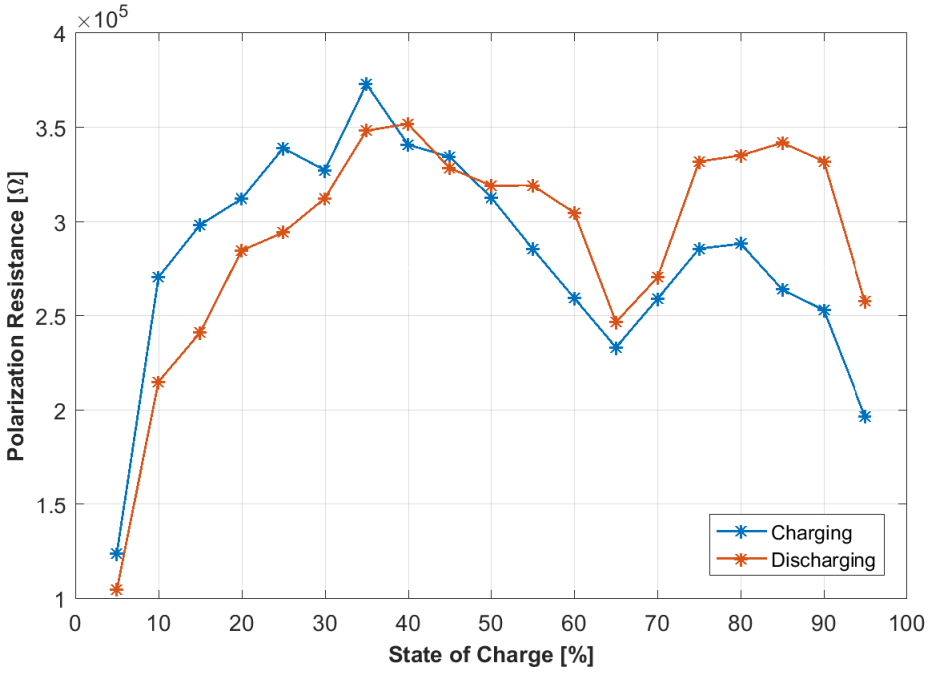

Figure 3-12 Equivalent capacitance during pulse charging and discharging of the battery cell at different SOC values (T=25 degC, 1C-rate)

3.1.2 Battery modelling

Usually, a battery cell is simulated using an equivalent electrical circuit modeled by large lookup tables representing each element of the circuit, as it was also presented in [37].

The electrical diagram of the circuit used in this project is illustrated in Figure 3-13. The open circuit voltage is SOC dependent and the EEC parameters are SOC and load current dependent.

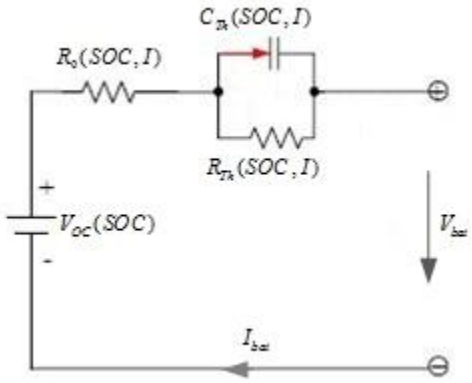

Figure 3-13 Equivalent circuit of the battery

Figure 3-14 depicts the block diagram of the modeled battery. It describes in detail the components of the equivalent electrical circuit, every block containing lookup tables populated with the data acquired in the previous section. This approach is perfectly suitable for model validation and verification, being able to simulate the terminal voltage. However, for this study a model which simulates power will be adjusted later.

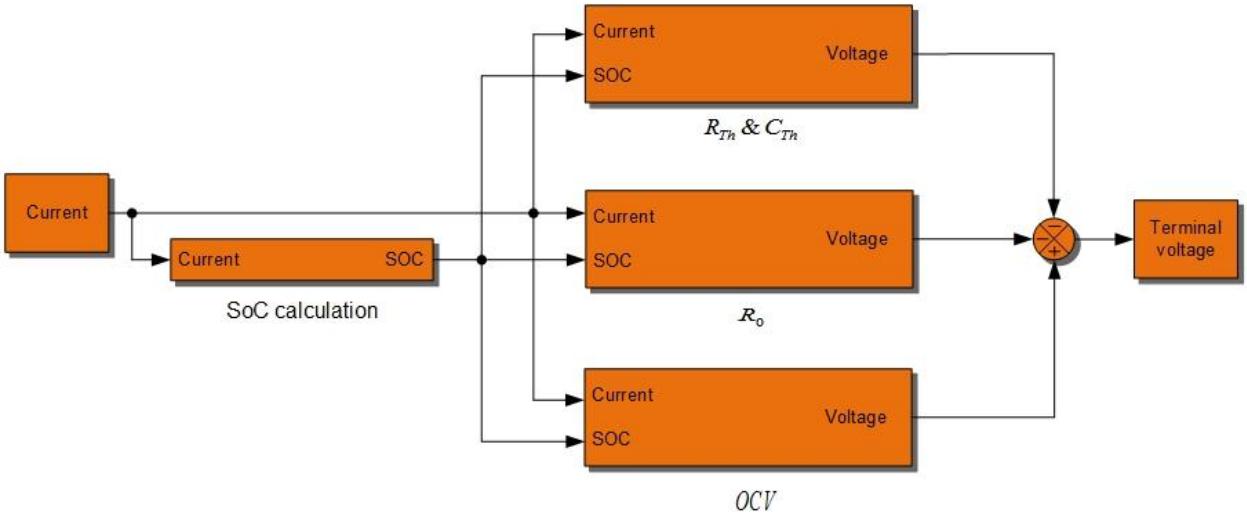

Figure 3-14 Block diagram of the modeled battery cell used for validation

The model simulates the terminal voltage of the battery following the next equation:

$$V_{bat} = V_{OC} \pm V_{EEC} \tag{12}$$

Where:

V_{bat} is the terminal voltage of the battery, measured in [V]; V_{OC} is the open-circuit voltage, measured in [V]; V_{EEC} is the internal resistance voltage, measured in [V].

The SOC calculation block uses the Coulomb counting method to estimate the SOC of the battery, and it is described by the equation below:

$$SOC = SOC_i - \frac{1}{Q} \times \int_{t_1}^{t_2} I_{bat} \times dt \tag{13}$$

Where:

SOC is the estimated state of charge, expressed in [%]; SOC_i is the initial state of charge, expressed in [%]; Q is the battery capacity during charging or discharging, measured in [Ah]; I_{bat} is the battery current, measured in [A].

3.1.3 Model validation

To evaluate the validity of the battery model, a current profile measured in laboratory (Figure 3-15) is adopted as an input for the lithium-ion battery model.

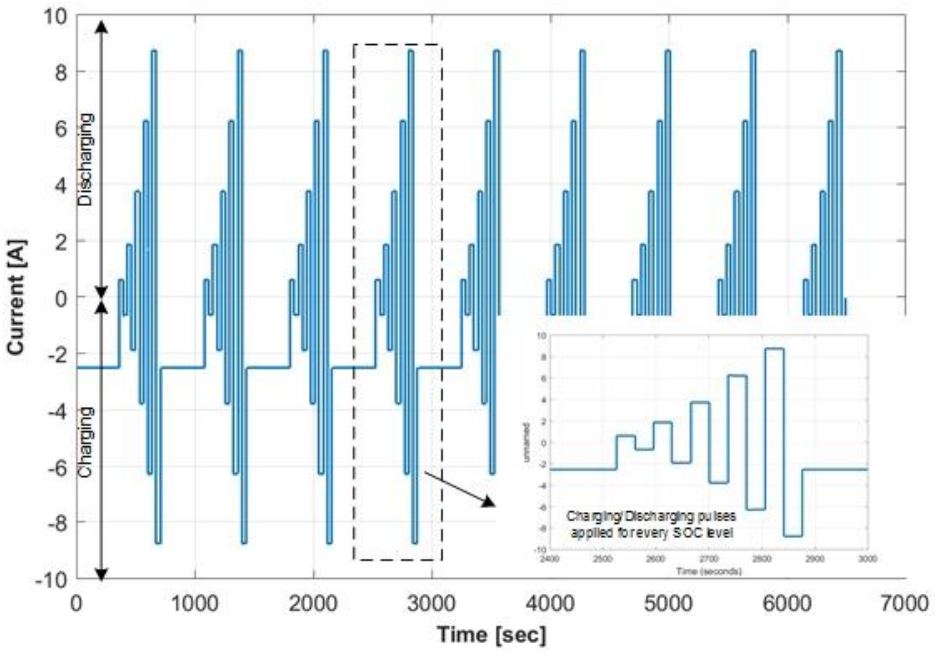

Figure 3-15 Current profile applied to the battery cell

The experimental steps for the current profile, can be seen in Figure 7-2, Appendix B.

In order to validate the model, a comparison of the measured and estimated voltage has been analyzed. In Figure 3-16, it can be seen both voltage profiles, with a slight offset of the modeled profile with respect to the measured one.

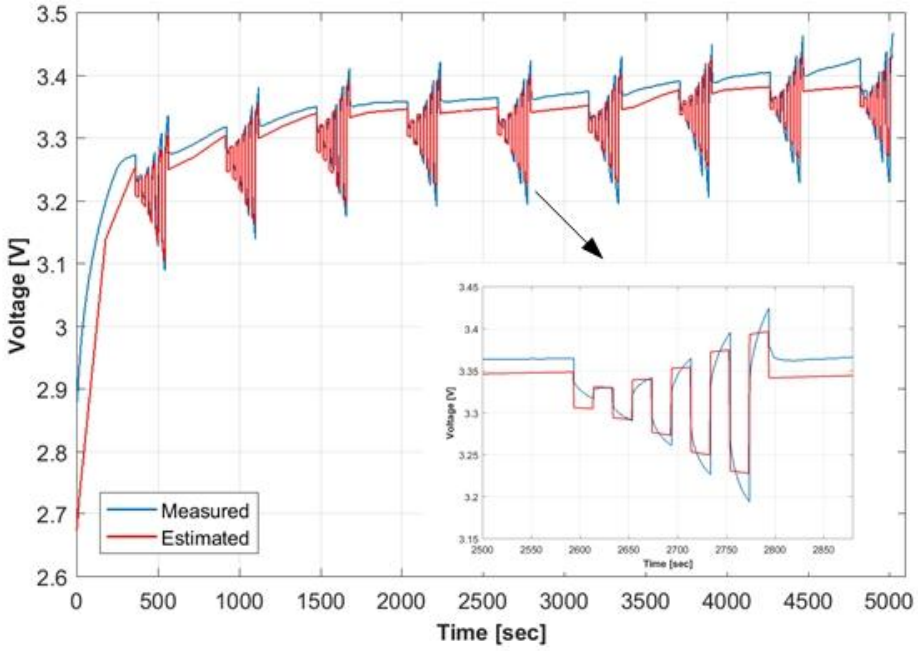

Figure 3-16 Comparison between measured voltage and estimated voltage of the battery cell

The estimated error of the modeled profile has been calculated following the equation below and it has been found to be 3%.

$$\text{error}[\%] = \frac{\text{abs}[\text{testSignal}(n) - \text{referenceSignal}(n)]}{\text{referenceSignal}(n)} \tag{14}$$

Where:

testSignal is the estimated voltage and referenceSignal is the measured voltage.

The verification of the model being satisfied, the modeled battery can be used in the project's studies. In order to have the desired rated power, 180 battery cells will be connected in series on a single branch. Simulations will be conducted for two battery sizes (6 kW and 3 kW). For the 6 kW battery, the charging current will be 4C (i.e. 10 A), which corresponds to a fully charged battery in 15 minutes. The 3 kW battery will be charged with 2C, the battery being fully charged in 30 minutes.

Furthermore, in this study being considered only the power, the battery model should be adjusted to have power as input/output, as it can be seen in Figure 3-17.

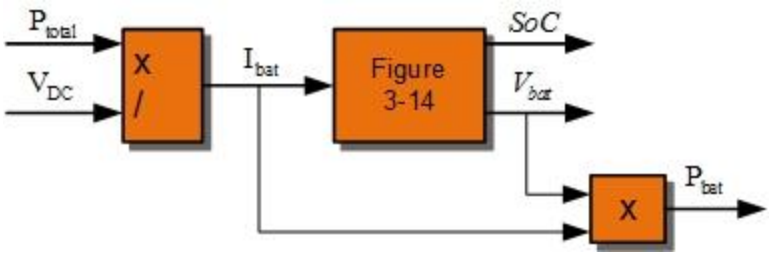

Figure 3-17 Block diagram of the battery storage

3.2 PV array performance model

The block diagram showed in Figure 3-18, illustrates the performance model of the solar PV that has been used in the current study.

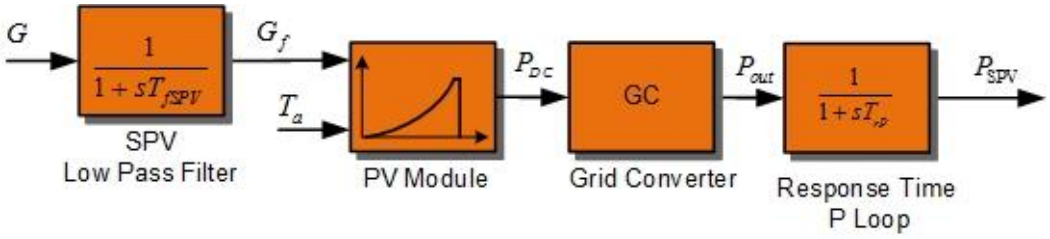

Figure 3-18 Block diagram of the solar PV system

The mathematical model of the PV generator is based on the parameters given in the datasheet (Table 9, Appendix C) of a real PV panel. The model ensures good accuracy and it is modeled according to [38].

The irradiance used in the model simulation is real data collected from Denmark, with a frequency bandwidth of maximum 5 Hz, hence, the irradiation time series will have a resolution of minimum 200 msec. A first order low pass filter is used to introduce smoother signals of solar irradiance.

Typically, the output power from a PV module mostly depends on the solar irradiance and the environmental temperature.

The PV module is connected to a grid converter, which matches the power losses of a real PV inverter, multiplying the power with an efficiency.

The response time of the active power injected into the grid is considered in the Point of Connection (PoC). Considered the small scale of the system, the response time is in the same range as the one in the low pass filter.

3.3 Wind turbine performance model

The block diagram showed in Figure 3-19, illustrates the performance model of the small wind turbine that has been used in the current report.

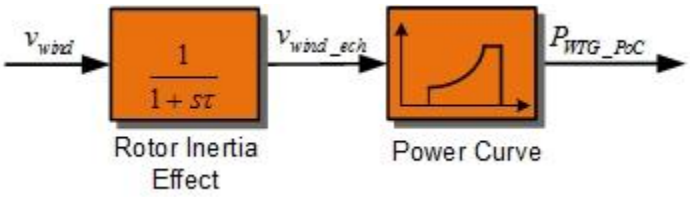

Figure 3-19 Block diagram of a simplified wind turbine

The turbine model is ideal for energy management studies and it is described by [39], [40] and [41].

The model has a bandwidth of maximum 1 Hz and can be used only for studies that require only the power output of the wind turbine.

The rotor inertia smoothens the time and position variability of the wind speed on the rotor plane. To capture the smoothening effect, a first order filter is considered. The parameters of the filter are calculated based on [39] and they are checked with data from [41].

The power curve of the wind turbine is showed in Figure 3-20 and it is certified for the Danish market according to [42]. The power curve relates the wind speed to the power production of the wind turbine as provided in the datasheet (Table 10, Appendix D).

Figure 3-20 Power curve of the 10 kW wind turbine [41]

4 Mission profile

4.1 Distributed generation power profiles

The models are based on real irradiance and wind speed data measured in Denmark. There have been considered two periods of the year, one day in summer and one day in winter, i.e. the irradiance and wind speed for a summer day have been measured starting with 25th of August until next day, and for a winter day, they have been measured starting with 25th of January until next day. The frequency bandwidth is 5 Hz, which implies that the solar irradiance and wind speed time series applied to the models will have a resolution of 200 msec. The curve profiles can be seen in the figures below (Figure 4-1 and Figure 4-2), together with the produced power.

During summer, the PV panels start to produce power earlier in the morning than during winter, and the irradiance level reaches almost 1200 W/m^2, and just 550 W/m^2 in winter season.

The wind speed is present almost all day during summer, and just half of the day in winter and the maximum speed reaches 10 m/s in both periods.

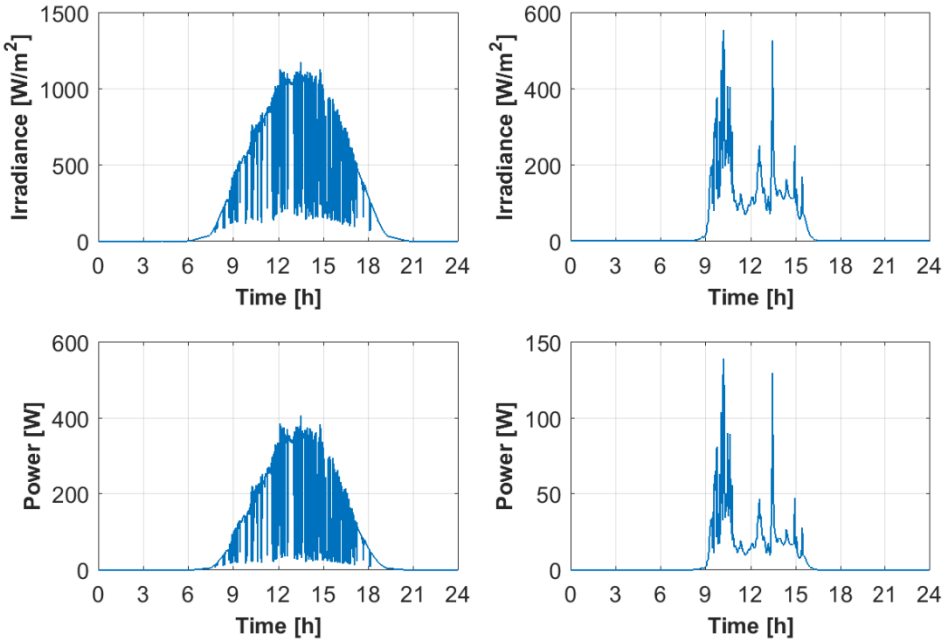

Figure 4-1 Input irradiance and PV power, during summer (left) and winter (right)

The power produced by photovoltaics and wind turbine depends significantly on the solar irradiance and wind speed, hence the same pattern of the curves, as it can be seen in Figure 4-1 and Figure 4-2.

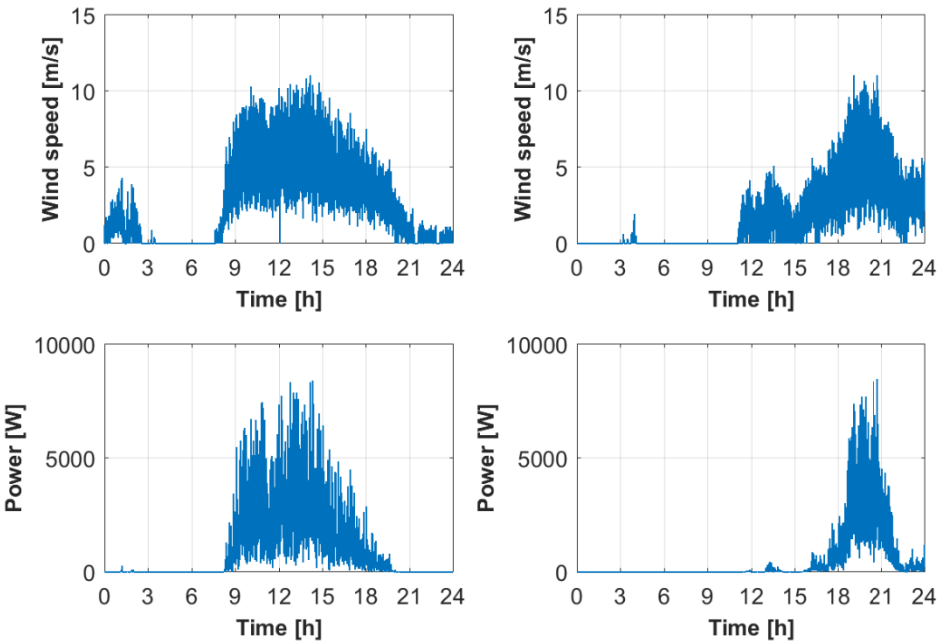

Figure 4-2 Input wind speed and WT power, during summer (left) and winter (right)

The power production from PVs reaches 400 W for the maximum irradiance in the summer and it hardly reaches 150 W in winter. The wind turbine produces power for half of the day during summer and just for a few hours during winter, the peak production reaching in both cases even 7500 W.

4.2 Demand profiles

The household consumption data used in this project is the domestic electrical consumption of a residential home, according to [43]. The total household consumption is randomly generated with the help of a graphical user interface (GUI) tool designed in [43].

Household's loads are different depending on the month and also depending on the day. Therefore, two periods of the year are considered, summer and winter, a day during weekday and one during weekend.

In the figures below it is shown the daily consumption among weekdays and weekends, in the two selected periods of the year. Therefore, Figure 4-3 illustrates the power consumption in a weekday, during summer (top) and winter (bottom) and Figure 4-4 illustrates the power consumption in a weekend day, during summer (top) and winter (bottom).

There is a significant difference between the power consumption during summer and winter. During winter, there is a higher consumption, because of the heating and lighting loads, the peak power reaching almost 4000 W. Also, more power is needed during peak hour periods, one in the morning and one in the evening.

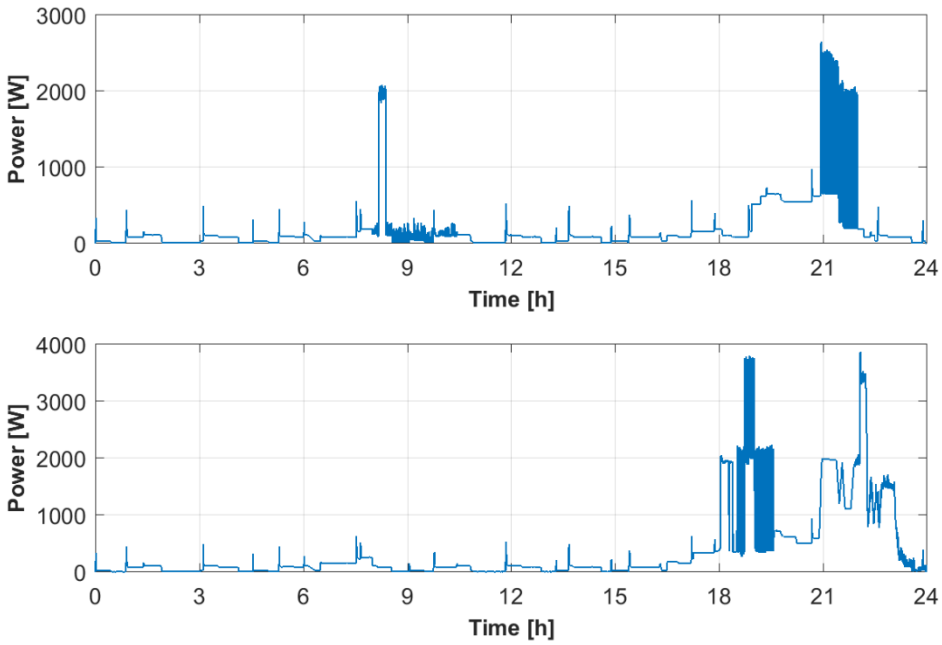

Figure 4-3 Household power consumption on a weekday, during summer (top) and during winter (bottom)

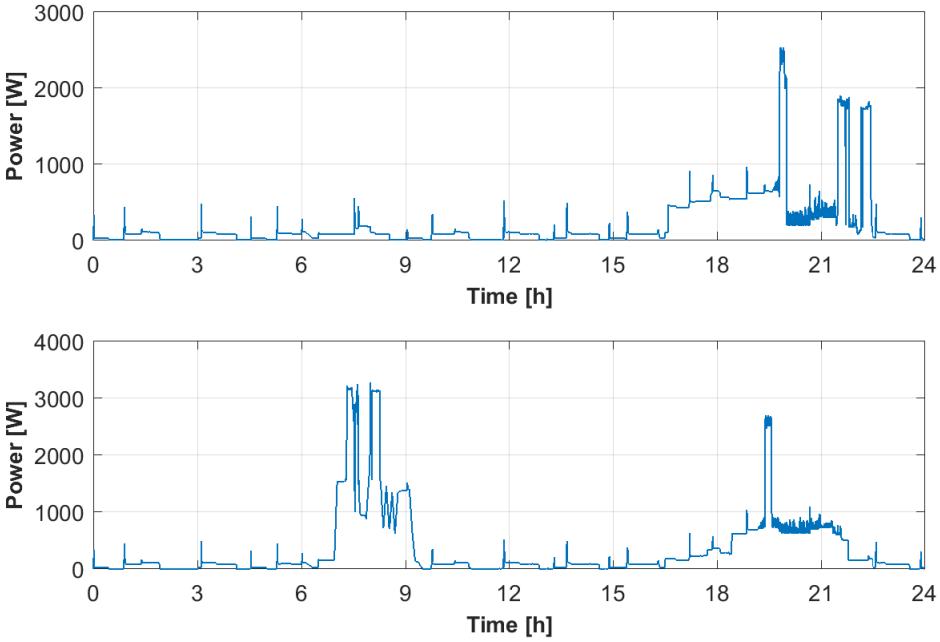

Figure 4-4 Household power consumption on a weekend day, during summer (top) and during winter (bottom)

5 Applications

5.1 Power smoothing

Moving clouds or changing in the wind speed behavior can yield to a fluctuating output power, as it can be seen in Figure 4-2. Furthermore, these fluctuations can cause power quality problems or other system instabilities. Therefore, before being injected into the utility grid, the power needs to be smoother. The proposed solution in order to smoothen the power is the integration of the battery with a power smoothing algorithm (Figure 5-1). In this paper, a simple moving average functionality (MAF) has been used to smooth out the noisy signal. The algorithm calculates the average of a given series of data in a fixed window size, the window being moved along the series and it is based on the equation below. The smoothing algorithm is configured to calculate a reference power signal of the produced power, that the system will try to track. The power difference between the power reference and the produced power will be used to control the charging and discharging of the BESS.

$$P_{grid}(t) = \frac{1}{T}\int_{t-T}^{t} [P_{hybrid}(t)dt \tag{15}$$

$$P_{hybrid}(t) = P_{PV}(t) + P_{WT}(t) \tag{16}$$

Where:

$P_{grid}(t)$ [W] is the smoothed power injected into the grid; T [s] is the moving average time window; $P_{hybrid}(t)$ is the total produced power [W], $P_{PV}(t)$ and $P_{WT}(t)$ are the time series output power from photovoltaics and wind turbine in [W].

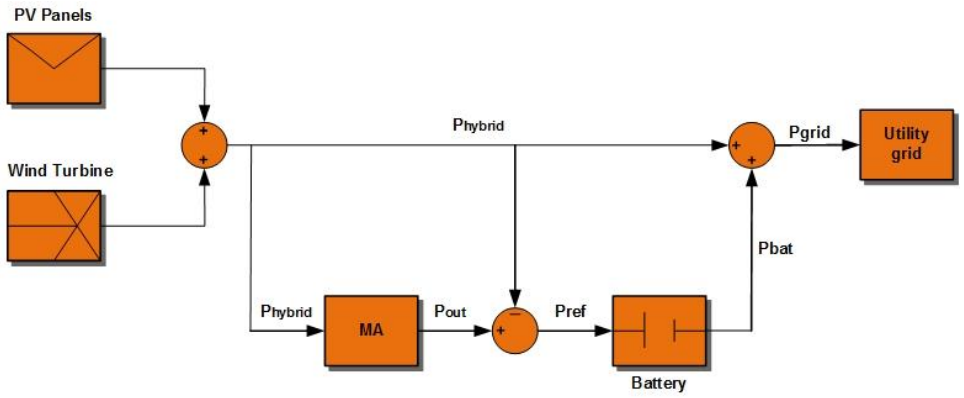

Figure 5-1 Block diagram of the power smoothing functionality strategy

In Figure 5-1, P_{hybrid} is the active power of photovoltaic panels and wind turbine; P_{out} is the target output, representing the output signal from the moving average algorithm; P_{ref} is the target signal for battery output; P_{bat} is the output power of the battery and P_{grid} is the total output after being smoothed.

The power smoothing service will be categorized into two cases with respect to the MA time window. The first case will simulate a 5-minute time window and the second case will simulate a 15-minute time window. Each case will be simulated with two different batteries, i.e. a 3 kW power battery and a 6 kW power battery, for two periods of the year, i.e. summer and winter.

5.1.1 6 kW battery energy storage

The first case simulates a 5-minute moving average (T=300 sec) for the smoothing function, during summer and winter period, using a 6 kW battery. The top plot (cyan color) from the simulation results figures includes the raw data representing the PV and WT power and the smoothed power (red color) corresponding to the actual power injected into the grid, which is the sum of the produced power and battery power. The left bottom plot represents the battery power (positive means that the battery supplemented power into the grid). The right bottom plot represents the SOC of the battery.

Moreover, comparisons between the target power and the grid power are illustrated in the figures below and an overview of the deviations between them can be seen in Table 1, at the end of this subchapter.

The smoothing effect of power fluctuations is obtained by charging and discharging the battery. In this process, if the hybrid power $P_{hybrid}(t)$, exceeds the expected output power, BESS will charge, and if the hybrid power is less than the expected power, BESS will discharge. If these two signals correspond, BESS will remain in floating charging state.

For the first case (T=300 seconds) during summer, when the power production is big and fluctuating, the smoothing algorithm together with the battery, is able to reduce the spikes, as it can be seen in the figures below. Also, the target power is perfectly tracked with a deviation of only 0.44%. The battery is able to achieve a 5-minute smoothing average by utilizing only a fraction of its capacity, SOC remaining at 50% without any deviation from the initial SOC. Because of the big amount of current transited through the battery during summer, there are 3 equivalent full cycles of the battery.

For the winter period, the same behavior takes place, the only difference being that the battery is less stressed, than in the summer period, with only one equivalent full cycle.

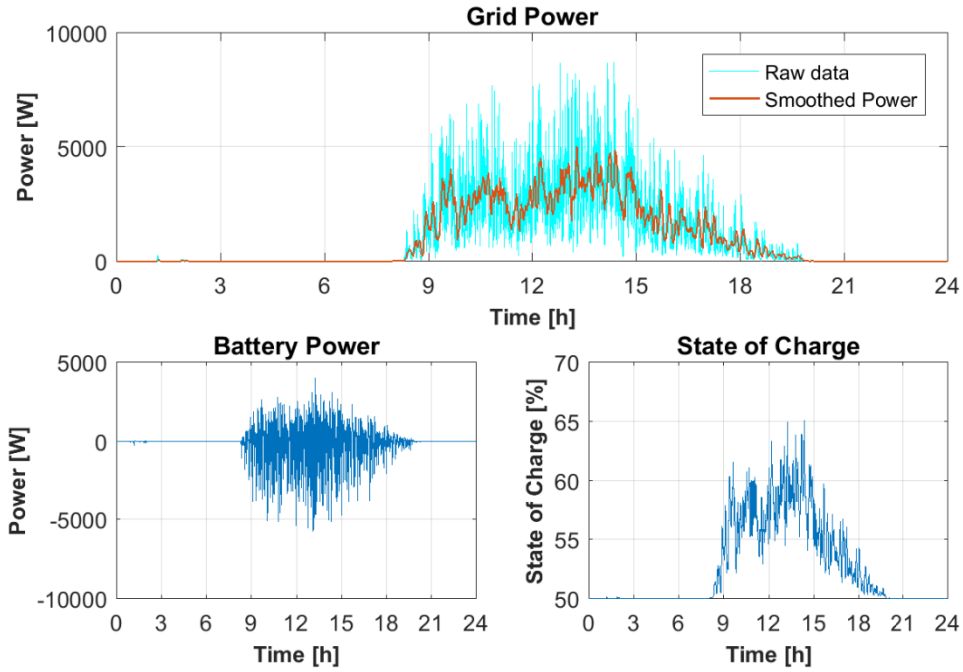

Figure 5-2 Simulation results of the first case (T=300 s, summer, 6 kW battery)

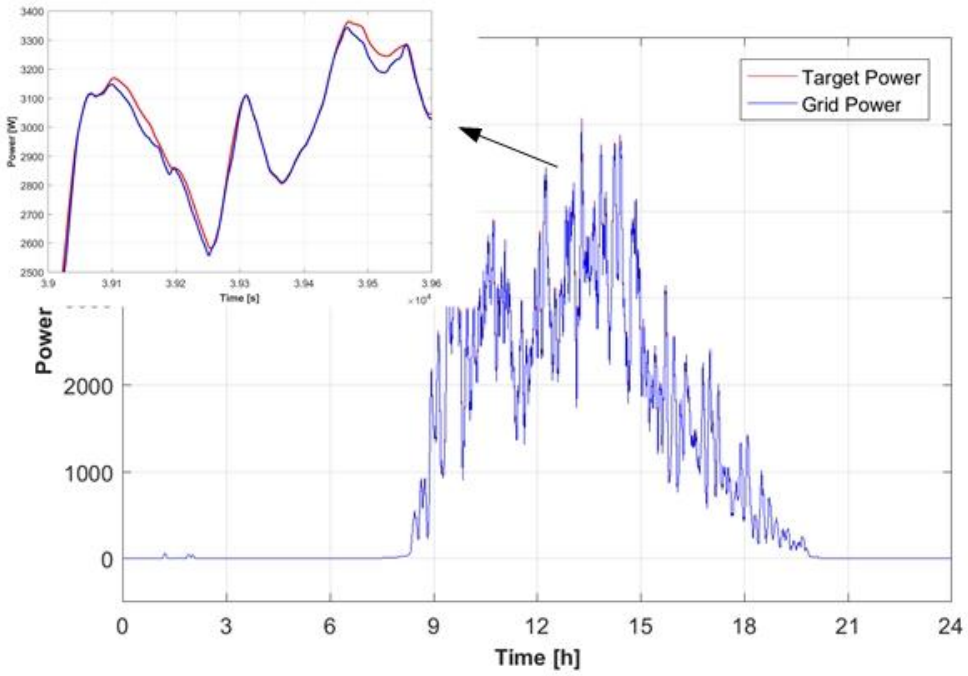

Figure 5-3 Comparison between the target power and grid power of the first case (T=300 s, summer, 6 kW battery)

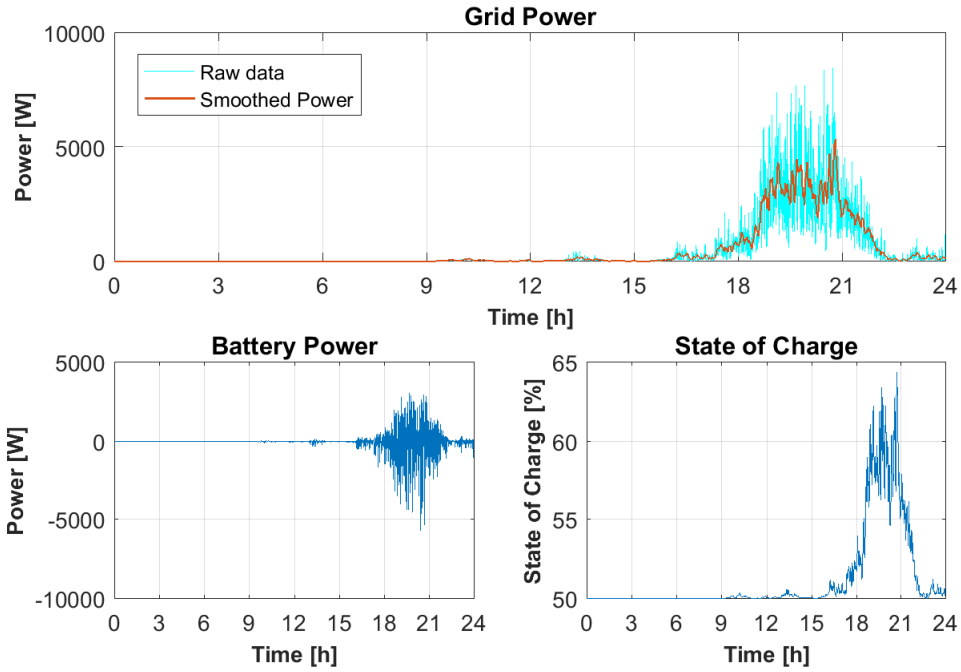

Figure 5-4 Simulation results of the first case (T=300 s, winter, 6 kW battery)

The second case is identical to the first case except that the time window of the average method increased to 15 minutes (T=900 seconds). The grid power is smoother, due to the greater MA time window, but the deviations between the target power and grid power are bigger. Also, SOC increases from 50% to 85% at the end of the day for both periods of the year.

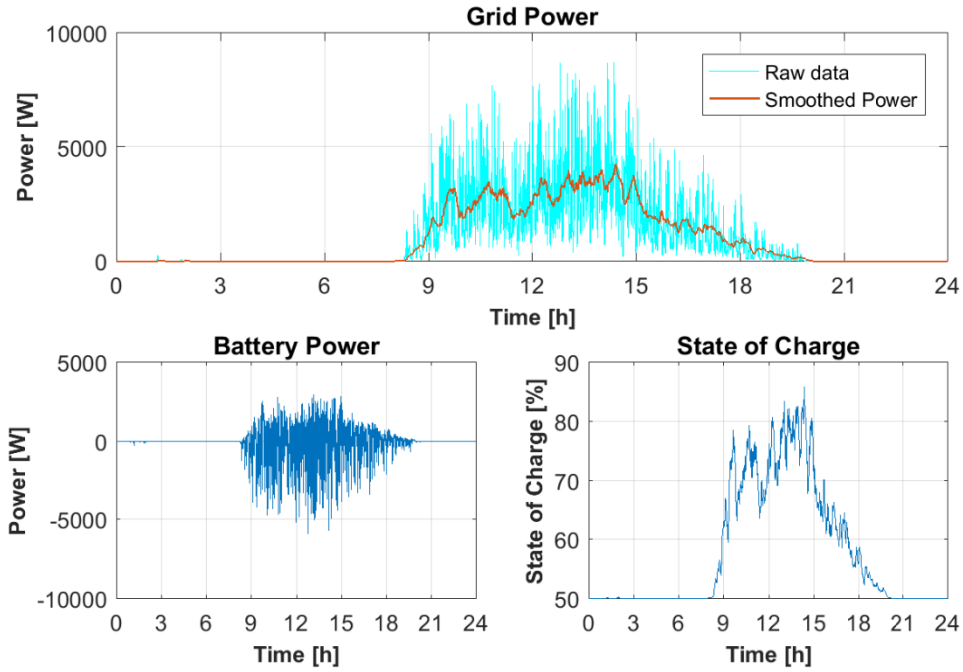

Figure 5-5 Simulation results of the second case (T=900 s, summer, 6 kW battery)

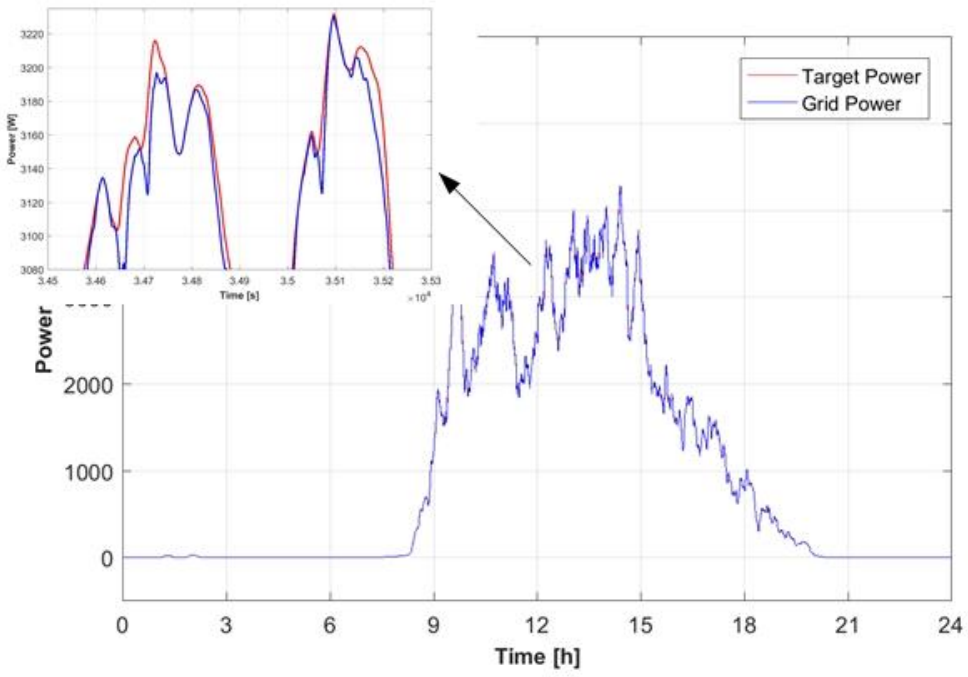

Figure 5-6 Comparison between the target power and grid power of the second case (T=900 s, summer, 6 kW battery)

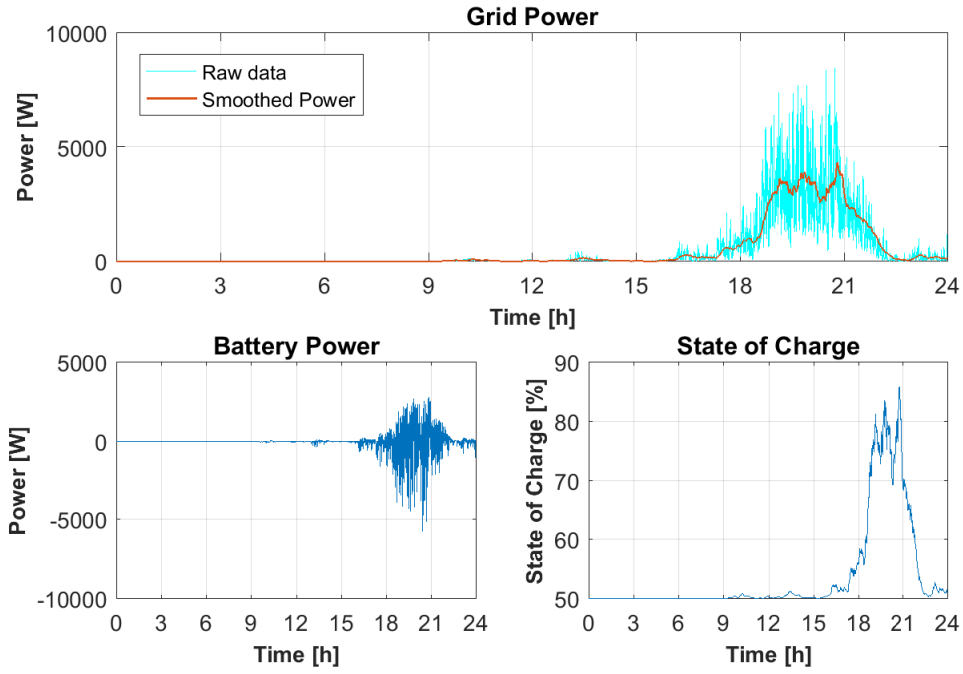

Figure 5-7 Simulation results of the second case (T=900 s, winter, 6 kW battery)

5.1.2 3 kW battery energy storage

For the smaller battery, the procedure is identical except that it is used a 3 kW battery in the smoothing process. The target power is being tracked successfully, with bigger deviations compared to the 6 kW battery. Also, SOC decreases in every case, due to the smaller size of the battery. Correspondingly, the number of full cycles is bigger for summer period, than for winter period, the battery having to charge/discharge a bigger amount of power during summer.

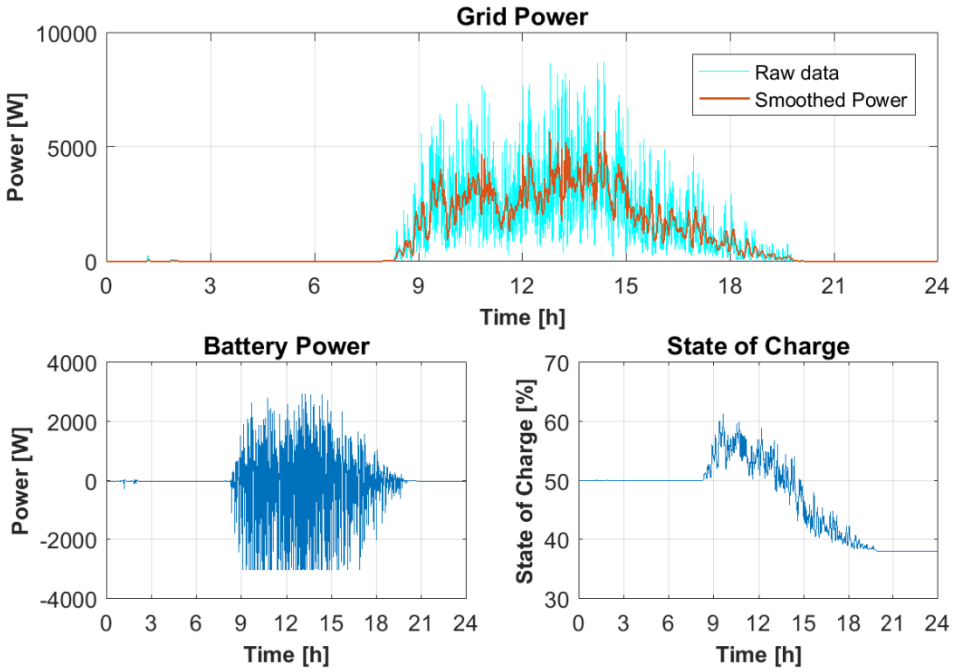

Figure 5-8 Simulation results of the first case (T=300 s, summer, 3 kW battery)

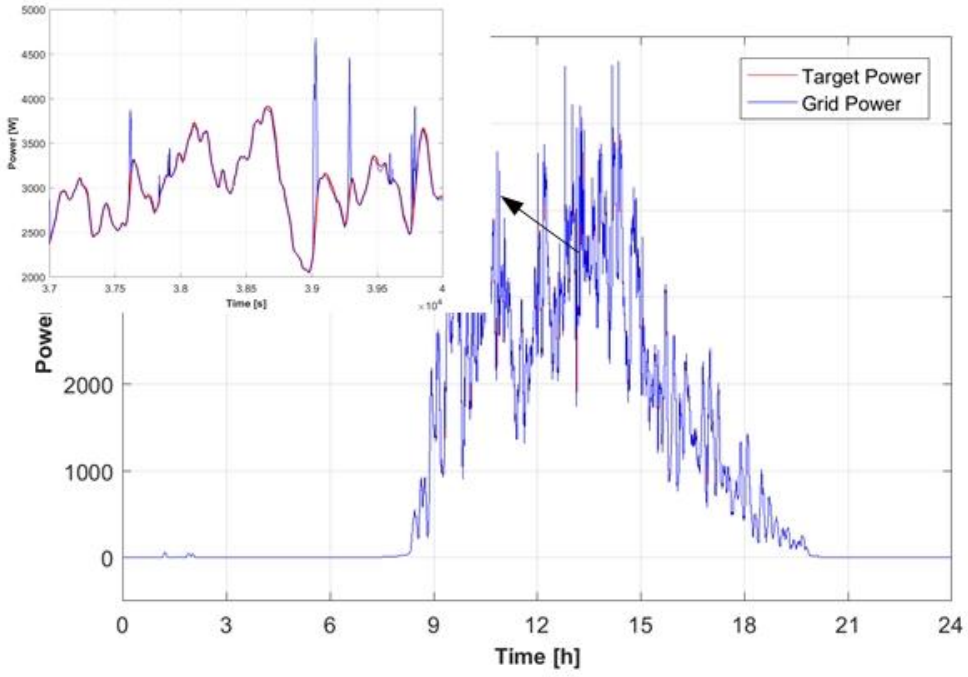

Figure 5-9 Comparison between the target power and grid power of the first case (T=300 s, summer, 3 kW battery)

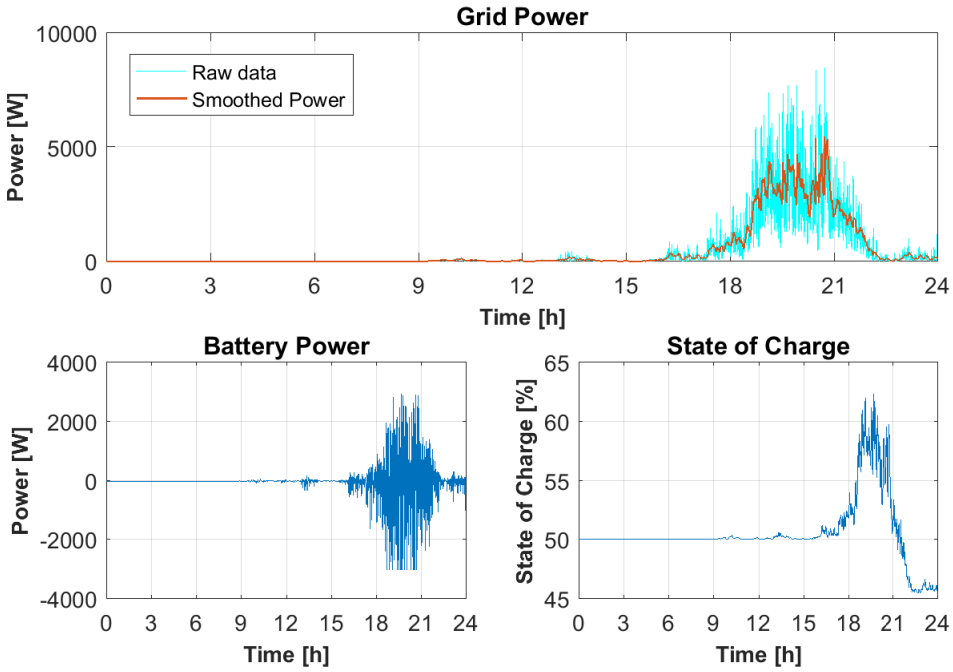

Figure 5-10 Simulation results of the first case (T=300 s, winter, 3 kW battery)

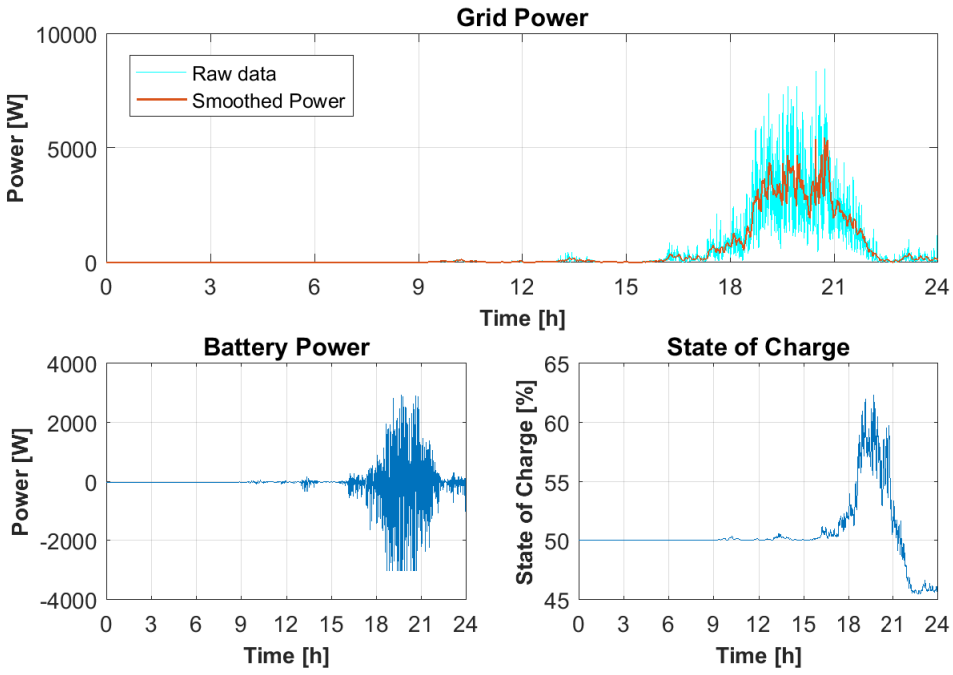

Figure 5-11 Simulation results of the second case (T=900 s, summer, 3 kW battery)

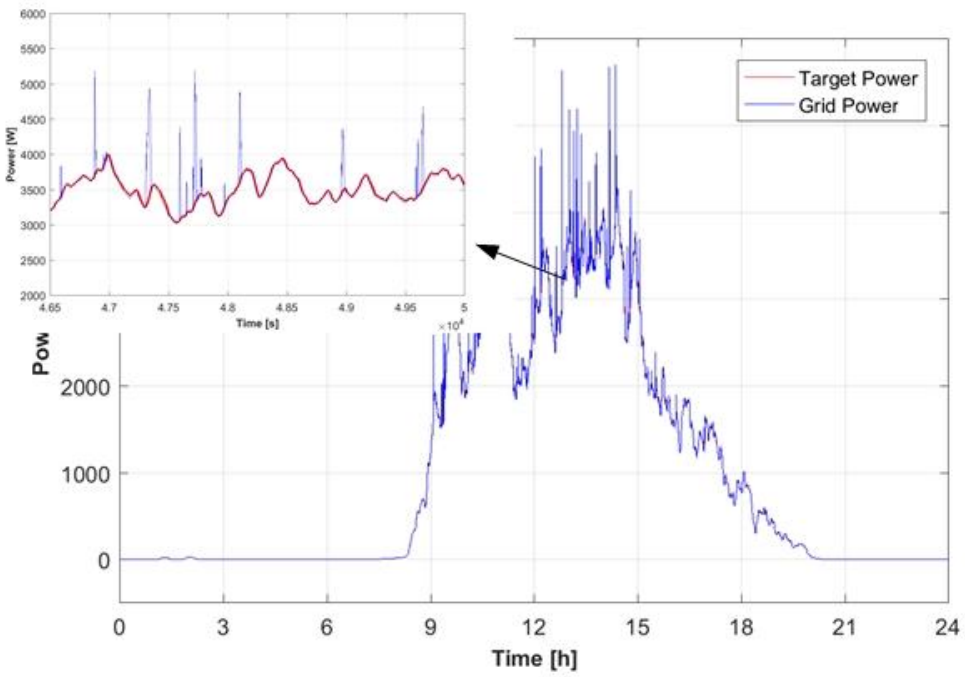

Figure 5-12 Comparison between the target power and grid power of the second case (T=900 s, summer, 3 kW battery)

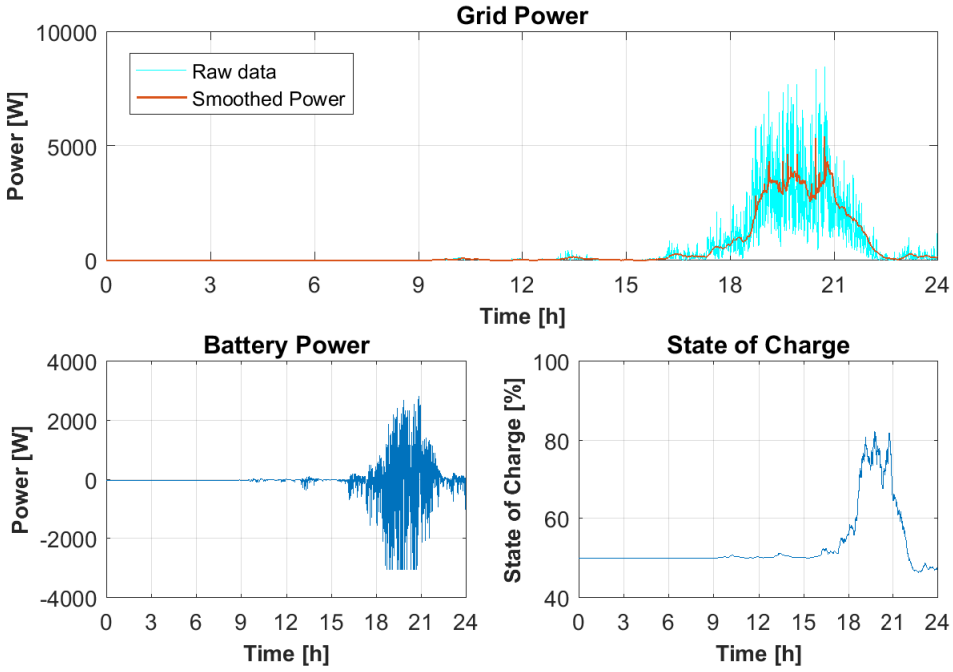

Figure 5-13 Simulation results of the second case (T=900 s, winter, 3 kW battery)

Table 1 Power smoothing deviations between the target power and the injected power

Period of the year	MA time window	Battery Power	
		3 kW	6 kW
Summer	5 min	0.76%	0.44%
	15 min	0.98%	0.72%
Winter	5 min	0.43%	0.33%
	15 min	0.67%	0.60%

Table 2 Battery response for power smoothing application

Power smoothing								
Battery Power	**3 kW**				**6 kW**			
Period of the year	Summer		Winter		Summer		Winter	
MA time window	5 min	15 min	5 min	15 min	5 min	15 min	5 min	15 min
min SOC [%]	38.03	37.58	45.48	46.46	50.00	50.00	50.00	50.00
max SOC [%]	61.29	78.08	62.36	82.38	65.11	85.85	64.36	85.83
Ah-throughput [Ah]	15.91	16.35	7.03	7.41	16.25	16.66	7.14	7.51
No. of full cycles [-]	3.20	3.27	1.41	1.48	3.25	3.33	1.43	1.50

5.2 Energy blocks

Energy storage systems have the flexibility to operate within the electricity market, and could improve the value of renewable energy.

The figures below (from Figure 5-14 to Figure 5-17) represent the typical power profiles of the residential home, for every period of the year/week, after the produced power has been extracted from the demand. The positive power curve corresponds to the power to be delivered and the negative power curve corresponds to the excess power.

The scope of this application is to minimize the amount of energy bought from the utility grid and sell a part of the excess production.

The proposed scheme is to calculate a 15-minute average (the red curve), representing the power that will be exchanged with the utility grid. The positive curve means that the power is bought and the negative curve means that the power is injected into the grid. The simulations will be conducted with a 3 kW and a 6 kW BESS.

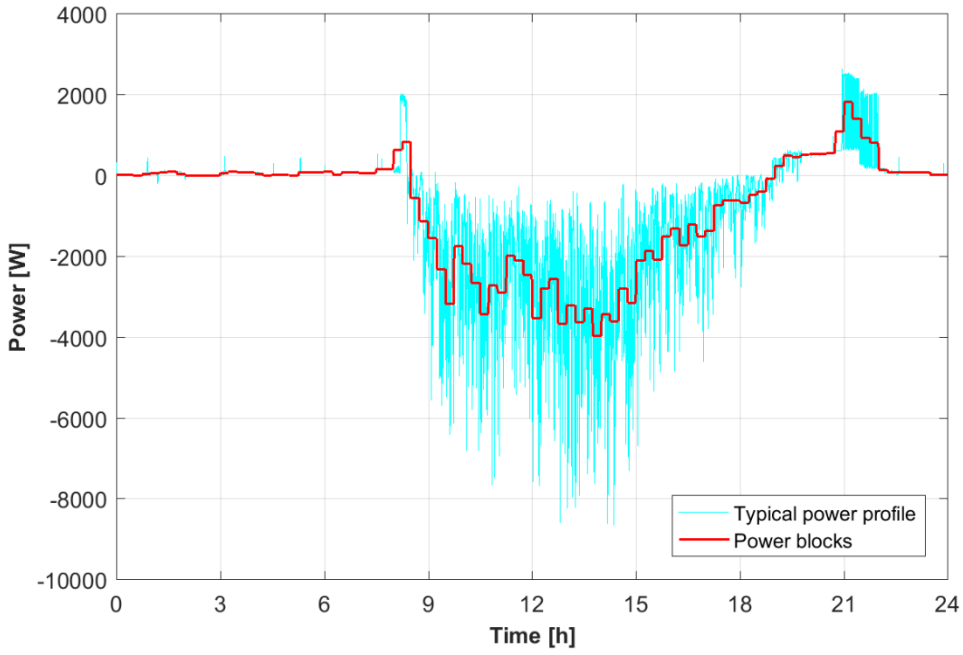

Figure 5-14 Overall power profile on a summer weekday

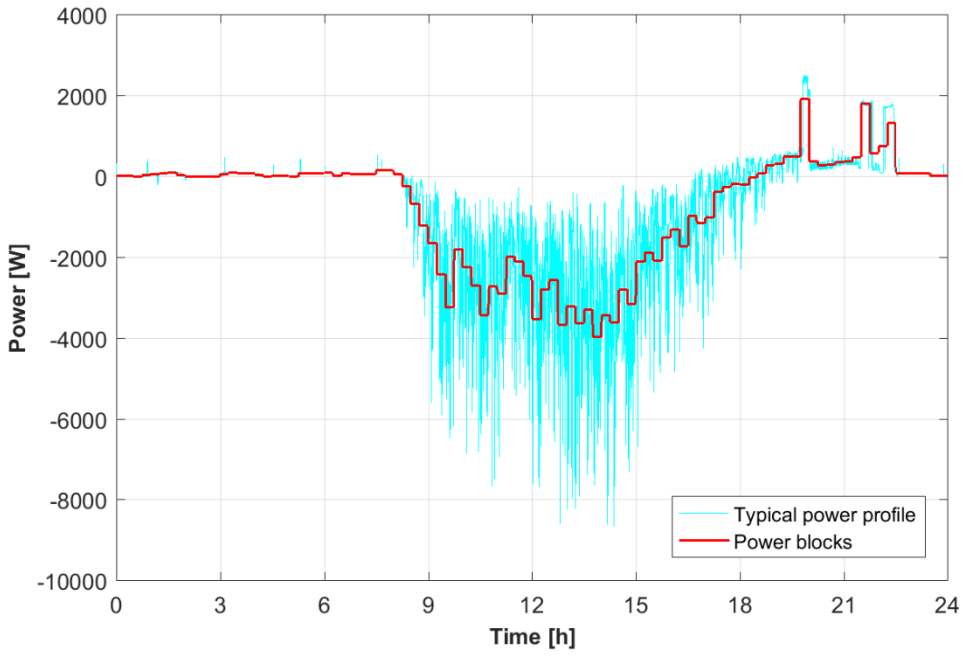

Figure 5-15 Overall power profile on a summer weekend

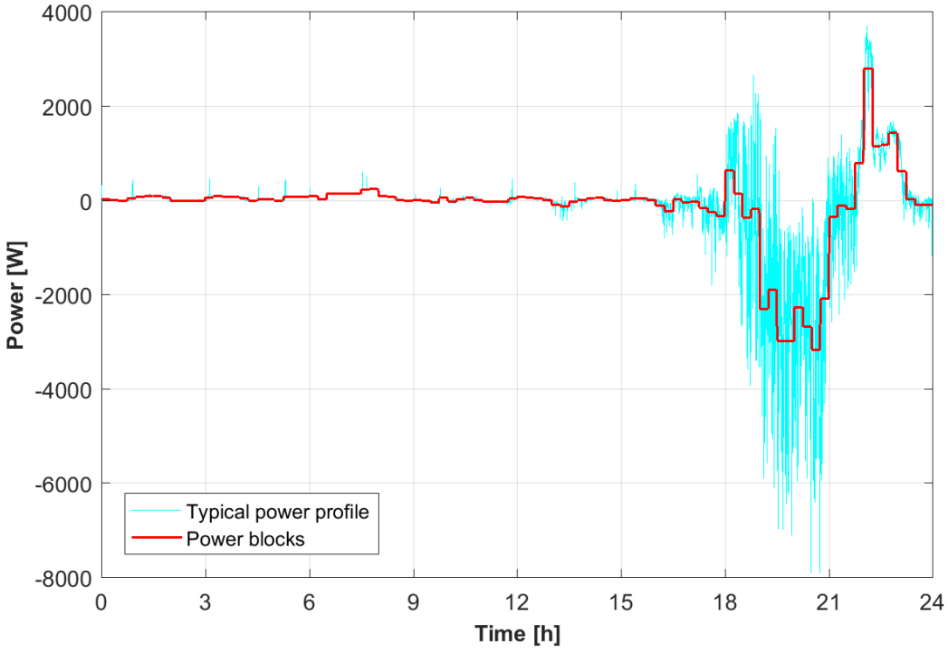

Figure 5-16 Overall power profile on a winter weekday

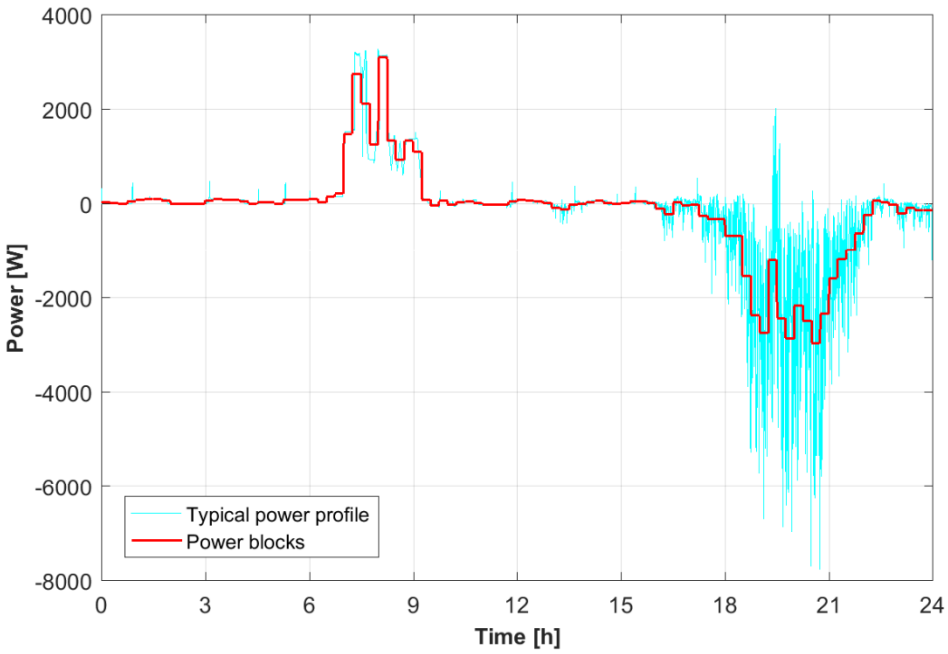

Figure 5-17 Overall power profile on a winter weekend

5.2.1 6 kW battery energy storage

The graphs below (from Figure 5-18 to Figure 5-21) illustrate the battery power request and the battery SOC. For the summer cases (Figure 5-18 and Figure 5-19), it can be seen that with an initial SOC of 50 %, at the end of the day the BESS manages to charge/discharge when the power exceeds the average limit, its SOC decreasing only a few percent because of the energy losses during charging/discharging. The number of equivalent full cycles reaches 4 cycles for this period, because of the large amount of the power charging and discharging the battery.

For winter cases (Figure 5-20 and Figure 5-21), the SOC at the end of the day remains nearly the same as the initial SOC (SOC at the start of the day), because of the lesser amount on energy floating through the battery, and there are 2 equivalent full cycles of the battery.

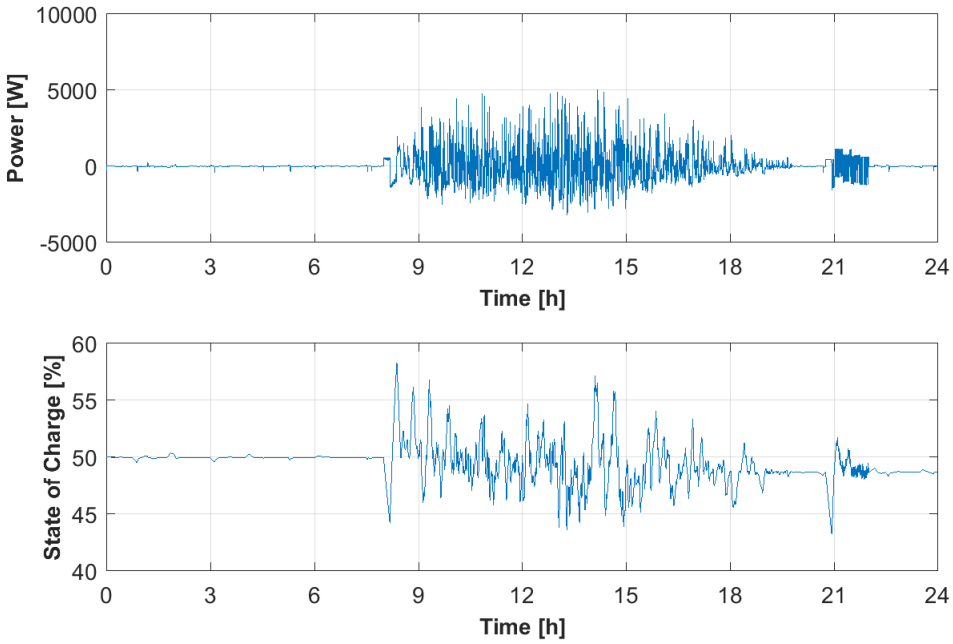

Figure 5-18 Battery power request on a summer weekday for a 6 kW battery

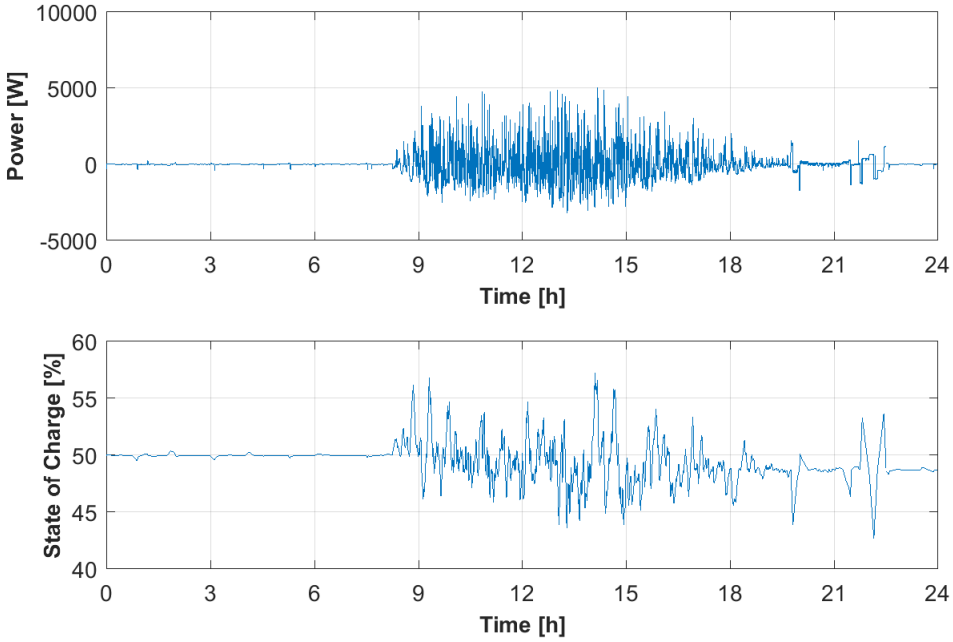

Figure 5-19 Battery power request on a summer weekend for a 6 kW battery

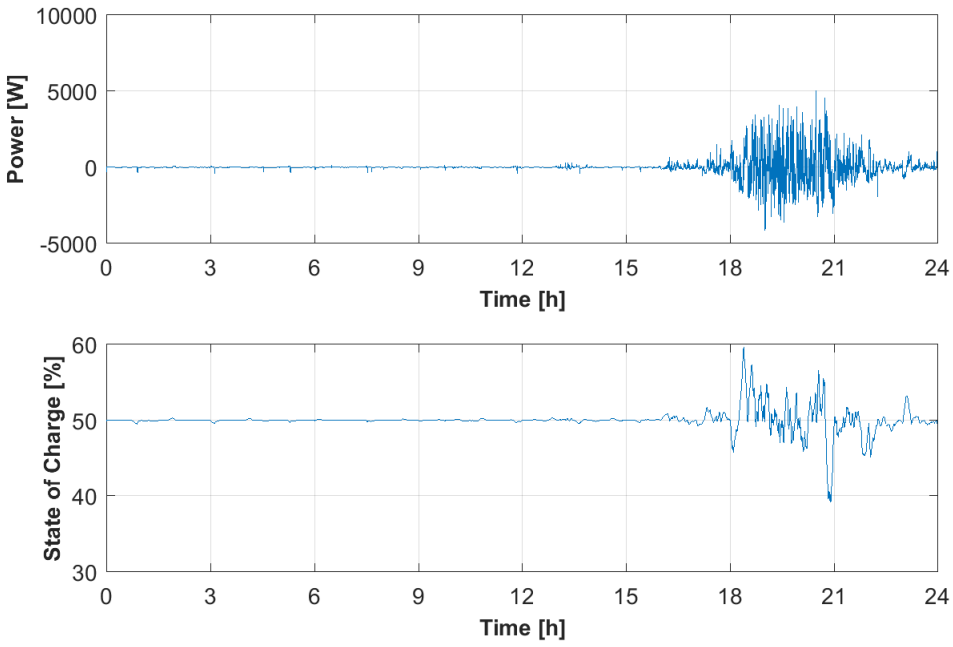

Figure 5-20 Battery power request on a winter weekday for a 6 kW battery

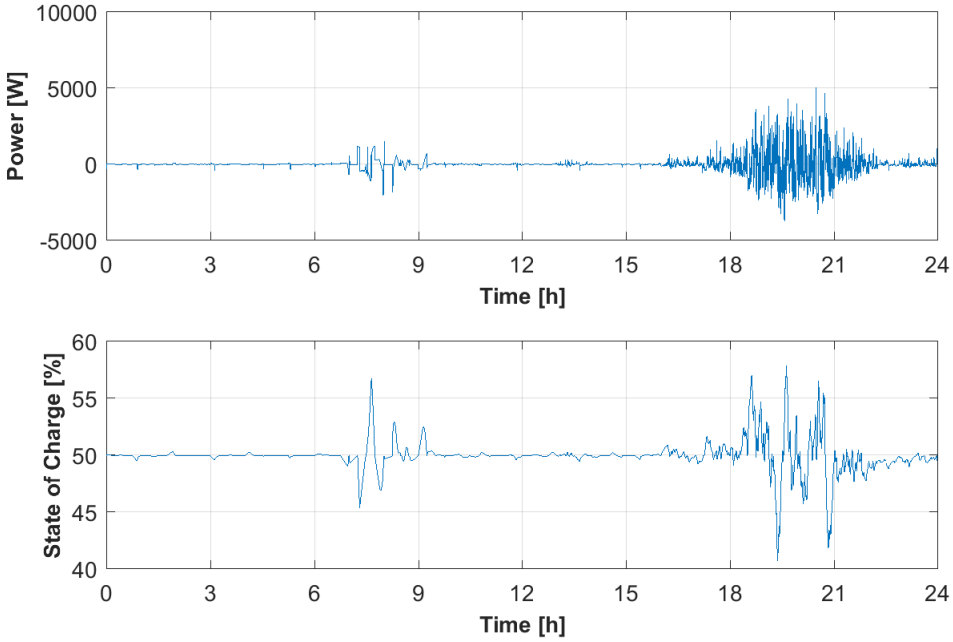

Figure 5-21 Battery power request on a winter weekend for a 6 kW battery

5.2.2 3 kW battery energy storage

For the smaller battery, it can be seen in the figures below (from Figure 5-22 to Figure 5-25) that its maximum power is reached for both summer and winter period, resulting in an increased SOC at the end of the day. During summer, there are 4, respectively 3, full equivalent cycles, for weekday and weekend, and only 2 full cycles for winter period.

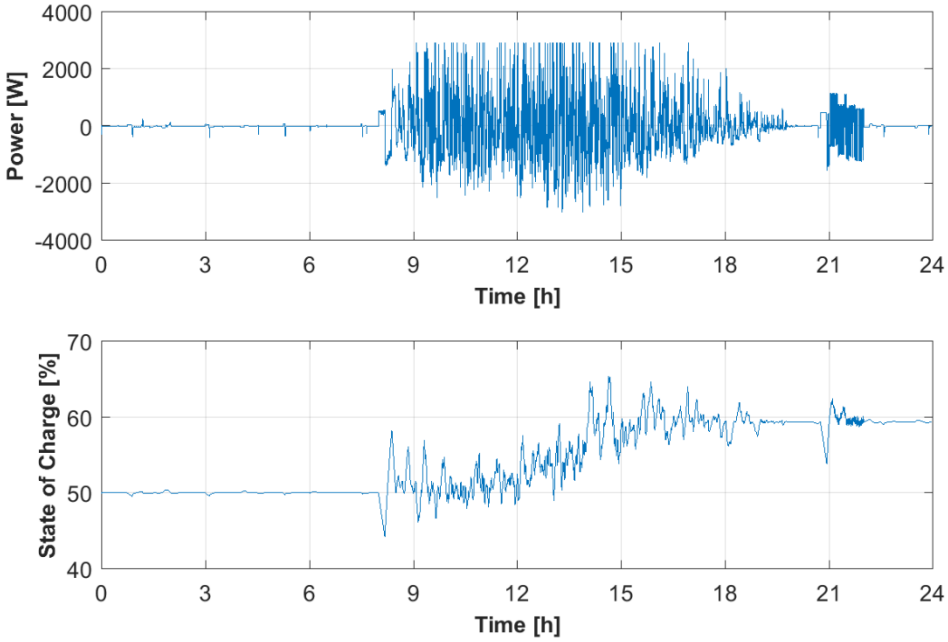

Figure 5-22 Battery power request on a summer weekday for a 3 kW battery

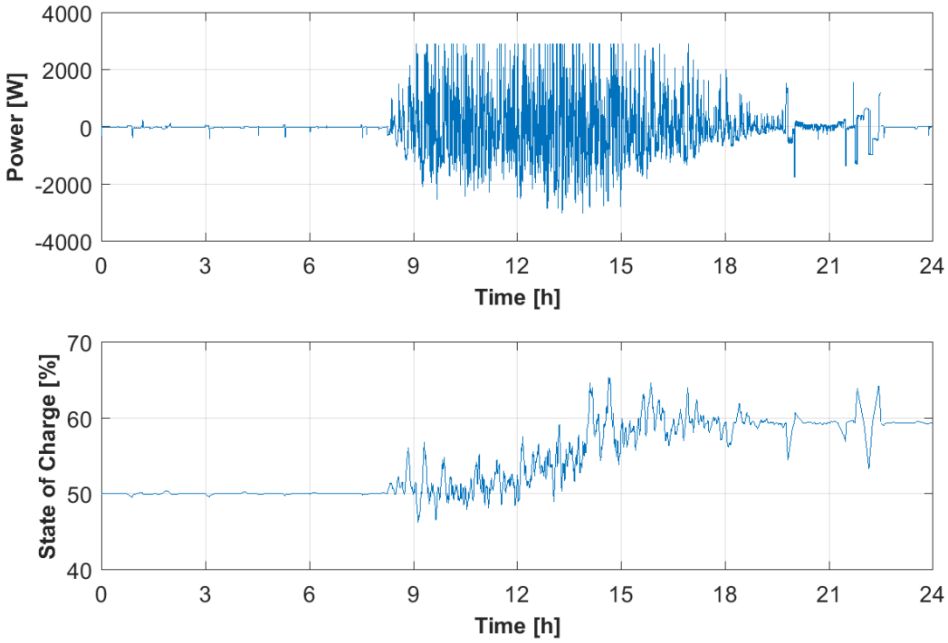

Figure 5-23 Battery power request on a summer weekend for a 3 kW battery

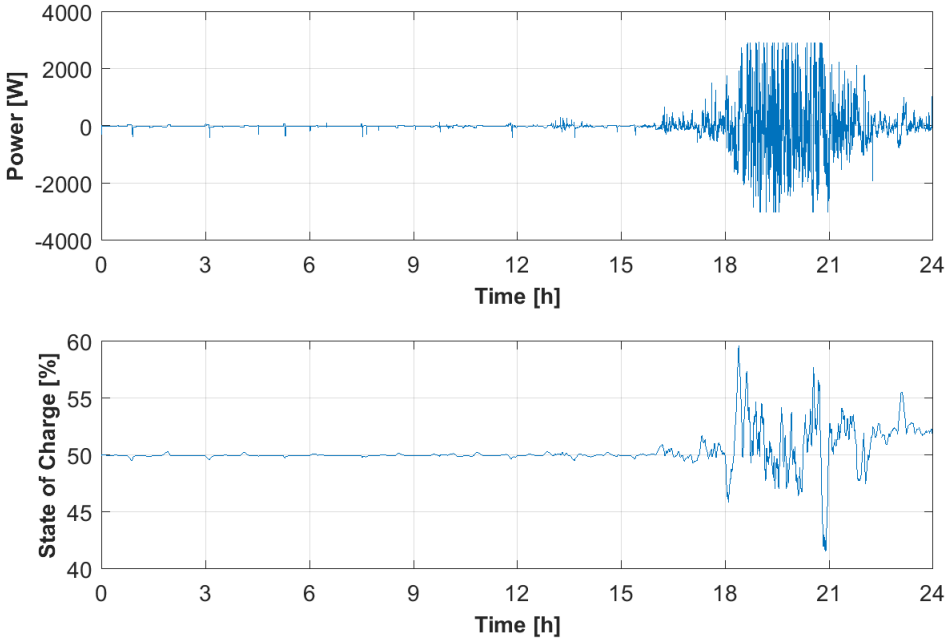

Figure 5-24 Battery power request on a winter weekday for a 3 kW battery

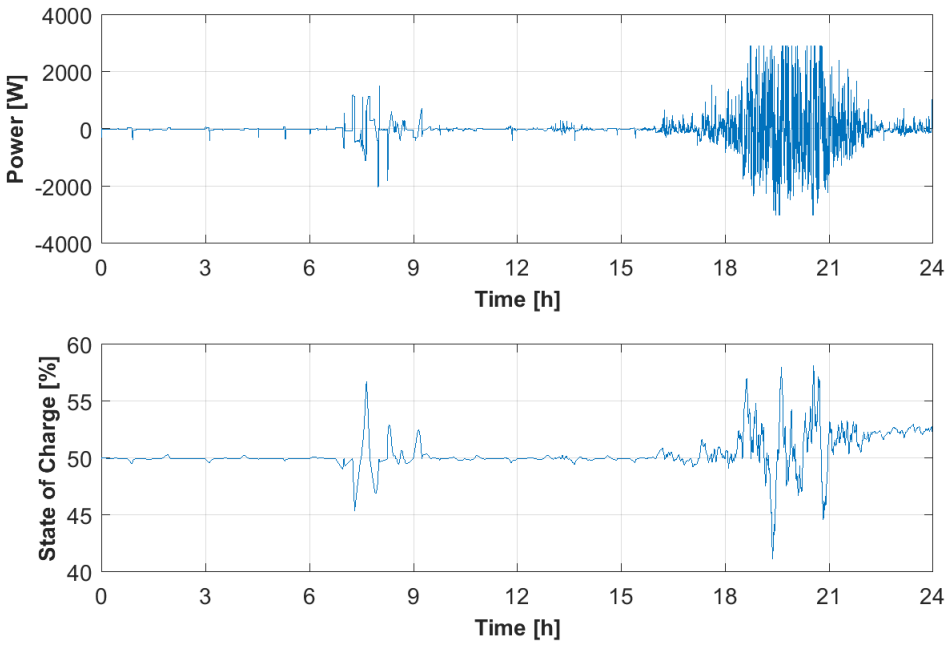

Figure 5-25 Battery power request on a winter weekend for a 3 kW battery

Table 3 Battery response for power blocks application

Power blocks								
Battery Power	**3 kW**				**6 kW**			
Period of the year	Summer		Winter		Summer		Winter	
Period of the week	weekday	weekend	weekday	weekend	weekday	weekend	weekday	weekend
min SOC [%]	44.23	46.28	41.52	41.18	43.26	42.66	39.18	40.73
max SOC [%]	65.43	65.44	59.63	58.18	58.32	57.22	59.63	57.86
Ah-throughput [Ah]	18.07	17.23	8.64	8.85	18.35	17.50	8.74	8.94
No. of full cycles [-]	3.61	3.45	1.73	1.77	3.67	3.50	1.75	1.79

6 Conclusion

In the current study a Lithium-ion battery has been modeled for a residential home with distributed generation from renewable resources. Battery energy storage systems are a suitable solution for renewable energy applications, due to their fast response and flexibility.

An accurate and comprehensive Li-ion battery performance model was proposed and parameterized for estimating the battery dynamic behavior. The model has been validated by comparing the simulation results with experimental data on Lithium-ion cell. The close accordance between the experiments and simulations shows that the proposed electrical model is satisfactory, being able to predict the voltage response within 3% error.

Battery energy storage systems have a short time response, being able to compensate the high variability of renewable resources. Therefore, BESS is used together with a moving average algorithm, to smoothen the power output by charging/discharging the battery in order to have a smoother power into the grid. Two different cases with respect to the MA algorithm time window have been analyzed, i.e. 5-minute and 15-minute window interval. Additionally, different periods of the year have been analyzed, since the PV production largely differs from winter to summer. Simulations with two different batteries show that the moving average strategy does not require big battery sizes, a 3 kW battery being able to smoothen the power fluctuations as well as a 6 kW battery. For all cases, the target power is correspondingly followed, with errors that do not exceed 1%. Furthermore, the battery has a greater cycling during summer, i.e. 3 full equivalent cycles, compared to only one full cycle during winter.

Further, BESS is used to maximize the usage of renewable energy and minimize the electricity bill. The scope of the scheme is to compute a 15-minute average power curve for the entire day, considering the house demand profile and the produced power, in order to minimize the bought power from the utility grid. The difference between the computed curve and the overall house power curve will be charged/discharged from the battery. For the 6 kW battery, the maximum power of the battery is never reached, and at the end of the day battery SOC corresponds to the initial SOC from the start of the day, i.e. 50%. Regarding the 3 kW battery, the maximum battery power is reached in every case, and at the end of the day battery SOC is increased. Similar to the first studied service (power smoothing), during summer the battery has approximately 4 or 3 complete cycles, and just 2 complete cycles during winter.

Finally, both battery sizes are suitable for power smoothing application, the grid power perfectly following the target power. For energy power blocks, a 6 kW battery is better recommended, because even when the production from renewable resources is reduced, a 3 kW battery would exceed its power limit.

The project goals have been achieved, the modeled battery energy storage system could provide suitable support for the studied renewable resources applications.

7 Future work

The conclusions of this project lead to several proposals for the future work.

- Studies with irradiance and wind speed data for one year;
- Studies with different battery technologies or other energy storage technologies;
- Battery lifetime analysis;
- Consider power grid topology and characteristics;
- Investigate other power fluctuations filtering methods;
- Assess economical aspect considering different financial payment schemes for residential users (cost of energy, investment return).

Appendices

Appendix A: Short market overview of home energy management systems

Table 4 HEMS products- market overview [20]

Company	Products	Product Category	Description
Whirlpool	Smart dishwasher/refrigerator/washer/dryer	Smart Appliance	It gives information about the status of the products and manages energy usage
Schneider Electric	Wiser In-Home Display	In-Home Display	It allows customers to monitor and control home energy usage through informative displays and color changing screens that alert users of changes in home energy usage and price.
Samsung	Family Hub Refrigerator, Wi-fi Range, Smart washer/dryer	Smart Appliance	-
Philips	Hue white and color, Hue Bloom, Hue Go, Hue LightStrip	Smart Lighting	Smart lighting with advanced control and color capabilities
NEEO	The NEEO Brain	Smart Hub	It commands the smart devices and gadgets. Works with Remote or mobile App.
LG	Smart ThinQ washer/dryer/refrigerator	Smart Appliance	It can detect when power consumption in the area is at its lowest, so the appliances can operate at lower energy rates
Green Energy Options	Energynote	Energy Portal	It visualizes and employs with the household consumption using an easy-to-use interface
GE	Link	Smart Lighting	Connected LED light bulb at a very affordable price.

Appendix B: Battery energy storage system

B1: Electrical parameters of the tested battery cell

Table 5 Electrical parameters of the tested battery cell

Capacity	Nominal Voltage	Max. Voltage	Min. Voltage	Max. Continuous Charge Current	Max. Continuous Discharge Current	Operating Temp.	Storage Temp.
[Ah]	[V]	[V]	[V]	[A]	[A]	[°C]	[°C]
2.5	3.3	3.6	2	10	70	-30 to 55	-40 to 60

B2: Capacity measurement values

Table 6 Charging and discharging capacity measured for all C-rates

	0.25C	0.5C	1C	2C	3C	4C
Charging Capacity [Ah]	2.5728	2.5815	2.5769	2.5735	2.5623	2.5572
Discharging Capacity [Ah]	2.5788	2.5775	2.572	2.5607	2.5555	2.5549

B3: OCV measurement values

Table 7 OCV vs. SOC

Charging		Discharging	
SOC [%]	**OCV [V]**	**SOC [%]**	**OCV [V]**
0	2.6664	0	2.6664
5	3.1125	5	3.1093
10	3.2204	10	3.202
15	3.2372	15	3.2171
20	3.2651	20	3.2363
25	3.2842	25	3.2523
30	3.2992	30	3.2641
35	3.3066	35	3.2818
40	3.3071	40	3.2915
45	3.3079	45	3.2927
50	3.3086	50	3.2937
55	3.3098	55	3.2947
60	3.3112	60	3.2967
65	3.3156	65	3.3002
70	3.3316	70	3.3169
75	3.3426	75	3.3339
80	3.3426	80	3.3347
85	3.3426	85	3.3355
90	3.3428	90	3.3365
95	3.3432	95	3.3397
100	3.4635	100	3.4635

B4: EEC parameters

Table 8 The EEC parameters for 0.1 C-rate

Charging					Discharging			
SOC [%]	**R0 [mΩ]**	**RTh [mΩ]**	**CTh [kF]**	**τ [min]**	**R0 [mΩ]**	**RTh [mΩ]**	**CTh [kF]**	**τ [min]**
5	3.04	22.16	435.26	160.75	8.80	15.20	923.67	234.00
10	8.00	10.80	1882.91	338.92	9.20	10.60	1950.05	344.51
15	9.20	10.40	2044.28	354.34	7.20	11.80	1584.42	311.60
20	7.60	10.00	2229.41	371.57	8.40	9.80	2316.19	378.31
25	9.60	8.00	3502.85	467.05	6.80	11.00	1848.49	338.89
30	8.00	9.20	2658.58	407.65	7.20	12.80	1370.25	292.32
35	8.40	8.00	3521.44	469.53	8.40	9.40	2544.63	398.66
40	9.20	7.60	3903.00	494.38	9.60	8.40	3187.16	446.20
45	8.40	10.00	2255.05	375.84	8.00	9.60	2440.95	390.55
50	9.20	8.00	3524.42	469.92	10.00	7.40	4108.90	506.76
55	8.80	8.80	2913.80	427.36	8.80	10.00	2250.97	375.16
60	6.40	11.20	1800.02	336.00	6.40	10.80	1931.24	347.62
65	10.00	9.60	2455.78	392.92	8.80	10.40	2087.15	361.77
70	10.80	8.00	3555.34	474.04	8.40	10.20	2181.52	370.86
75	9.20	9.60	2472.67	395.63	7.20	10.20	2184.72	371.40
80	8.80	9.60	2472.67	395.63	7.60	10.20	2184.79	371.41
85	9.60	8.80	2943.21	431.67	8.00	10.80	1949.02	350.82
90	9.20	8.80	2944.35	431.84	7.60	11.20	1812.65	338.36
95	9.20	10.80	1958.70	352.57	8.40	11.40	1752.26	332.93

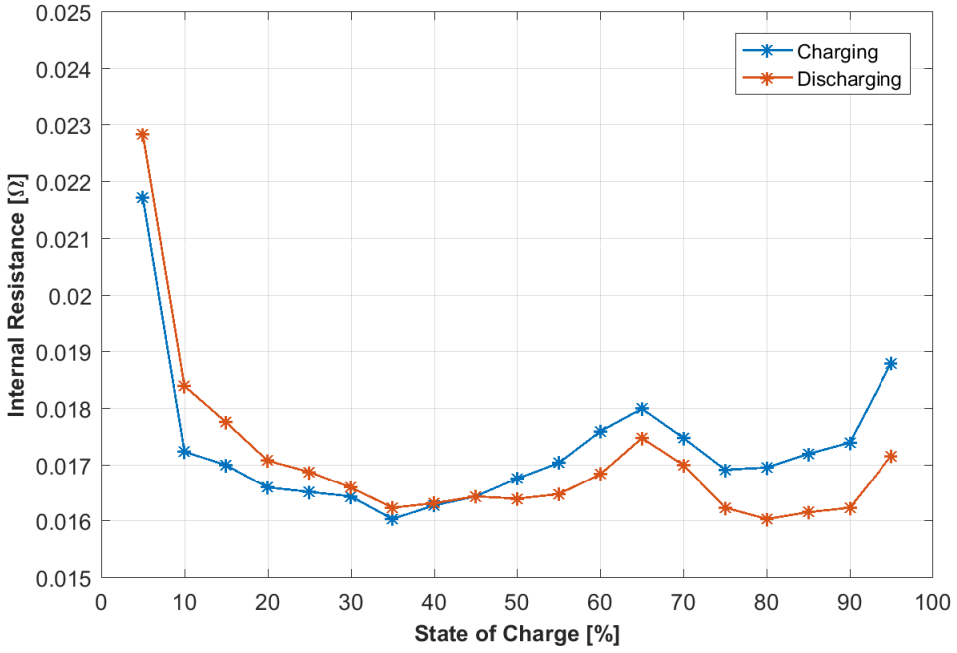

Figure 7-1 Internal resistance during pulse charging and discharging of the battery cell at different SOC values (T=25 degC, 1C-rate)

B5: The current profile applied to the battery during the verification of the performance model

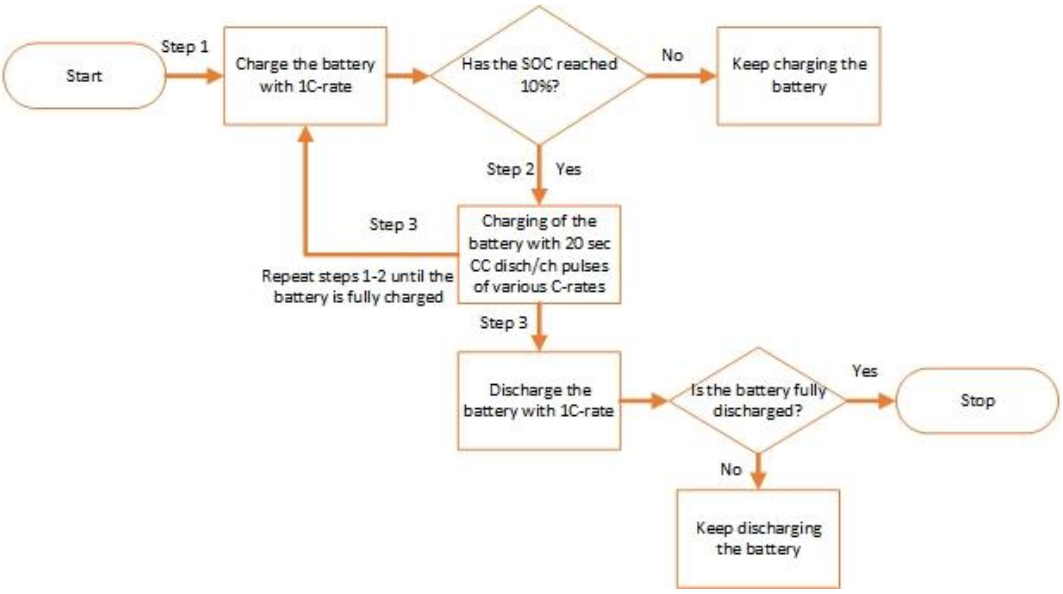

Figure 7-2 Steps of the applied current to the battery cell during the verification of the performance model

Appendix C: Solar photovoltaic system

C1: Parameters of the solar PV

Table 9 Parameters of the solar PV in STC [44]

Rated Power	Total Installed Power	No. of PV Panels	Vm	Voc	Im	Isc	NOCT	Module efficiency
[W]	[W]	[-]	[V]	[V]	[A]	[A]	[K]	[%]
360	6120	17	38.4	48.3	9.39	9.84	318	18.4

Appendix D: Wind turbine system

D1: Parameters of the wind turbine

Table 10 Parameters of the wind turbine [41]

Rated Capacity	Start-up Wind Speed	Rated Wind Speed	Survival Wind Speed	Rotor Diameter
[kW]	[m/s]	[m/s]	[m/s]	[m]
10	2.5	9.5	50	9.7

Bibliography

[1] IRENA, *Planning for the Renewable Future*. 2017.

[2] International Energy Agency (IEA), “CO2 Emissions from Fuel Combustion,” *Energy Technol. Anal.*, no. OECD/IEA, Paris, p. 533, 2009.

[3] P. Glanville, *Letting in the Light: How Solar Photovoltaic will Revolutionise the Electricity System*, no. 575. 2016.

[4] IRENA, “No Title.” [Online]. Available: www.irena.org.

[5] J. M. Savino, “Wind power,” *October*, vol. 2008, no. March, p. 299, 1975.

[6] IRENA, “Market Overview,” *Brazil Def. Secur. Rep.*, no. 2, pp. 64–69, 2012.

[7] EUROBAT, EHPA, and SolarPower Europe, “Solar and Storage,” 2016. [Online]. Available: https://eurobat.org/sites/default/files/solar_and_storage_position_paper_2016_1.pdf.

[8] IRENA, “Battery Storage for Renewables : Market Status and Technology Outlook,” *Irena*, no. January, p. 60, 2015.

[9] G. Huff, A. B. Currier, B. C. Kaun, D. M. Rastler, S. B. Chen, D. T. Bradshaw, and W. D. Gauntlett, “DOE/EPRI 2013 electricity storage handbook in collaboration with NRECA,” *Rep. SAND2013- …*, no. July, p. 340, 2013.

[10] Energy Storage Association, “Energy Storage Association.” [Online]. Available: http://energystorage.org/.

[11] P. Komor and J. Glassmaire, “Electricity Storage and Renewables for Island Power,” *Irena*, no. May, p. 48, 2012.

[12] B. Zhou, W. Li, K. W. Chan, Y. Cao, Y. Kuang, X. Liu, and X. Wang, “Smart home energy management systems: Concept, configurations, and scheduling strategies,” *Renew. Sustain. Energy Rev.*, vol. 61, pp. 30–40, 2016.

[13] IEA, “Photovoltaic power systems annual report 2015.”

[14] Energinet.dk, “Danish national transmission system operator.” [Online]. Available: energinet.dk.

[15] Energistyrelsen, “Danish Energy Agency.” [Online]. Available: ens.dk.

[16] Energinet.dk, “Annual Report 2015,” p. 72, 2015.

[17] G. Winkler, “Intelligent energy management of electrical power systems with distributed feeding on the basis of forecasts of demand and generation,” *16th Int. Conf. Exhib. Electr. Distrib. (CIRED 2001)*, vol. 2001, no. CP482, pp. v4-31-v4-31,

2001.

[18] S. Weitemeyer, D. Kleinhans, T. Vogt, and C. Agert, “Integration of Renewable Energy Sources in future power systems: The role of storage,” *Renew. Energy*, vol. 75, pp. 14–20, 2015.

[19] NEEP, “Opportunities for Home Energy Management Systems (HEMS) in Advancing Residential Energy Efficiency Programs,” no. August, 2015.

[20] NEEP, “HEMS Technology Assessment.” [Online]. Available: http://www.neep.org/initiatives/high-efficiency-products/home-energy-management-systems.

[21] H. Ghoddami, M. B. Delghavi, and A. Yazdani, “An integrated wind-photovoltaic-battery system with reduced power-electronic interface and fast control for grid-tied and off-grid applications,” *Renew. Energy*, vol. 45, pp. 128–137, 2012.

[22] M. Salameh, “Analysis of the Effects of a Passing Cloud,” *Ieee Trans.*, vol. 14, no. 4, pp. 1572–1577, 1999.

[23] T. Lipman, R. Ramos, and D. Kammen, *An Assessment Of Battery And Hydrogen Energy Storage Systems Integrated With Wind Energy Resources In California*, no. September. 2005.

[24] O. C. Onar, M. Uzunoglu, and M. S. Alam, “Modeling, control and simulation of an autonomous wind turbine/photovoltaic/fuel cell/ultra-capacitor hybrid power system,” *J. Power Sources*, vol. 185, no. 2, pp. 1273–1283, 2008.

[25] A. Hajizadeh and M. A. Golkar, “Intelligent power management strategy of hybrid distributed generation system,” *Int. J. Electr. Power Energy Syst.*, vol. 29, no. 10, pp. 783–795, 2007.

[26] M. Chen and G. A. Rincón-Mora, “Accurate electrical battery model capable of predicting runtime and I-V performance,” *IEEE Trans. Energy Convers.*, vol. 21, no. 2, pp. 504–511, 2006.

[27] M. R. Jongerden and B. R. Haverkort, “Which battery model to use?,” *IET Softw.*, vol. 3, no. 6, p. 445, 2008.

[28] O. Erdinc, B. Vural, and M. Uzunoglu, “A dynamic lithium-ion battery model considering the effects of temperature and capacity fading,” *2009 Int. Conf. Clean Electr. Power, ICCEP 2009*, pp. 383–386, 2009.

[29] M. Swierczynski, D. I. Stroe, A. I. Stan, R. Teodorescu, and D. U. Sauer, “Selection and performance-degradation modeling of limo2/li 4ti5o12 and lifepo4/c battery cells as suitable energy storage systems for grid integration with wind power plants: An example for the primary frequency regulation service,” *IEEE Trans. Sustain. Energy*, vol. 5, no. 1, pp. 90–101, 2014.

[30] V. Johnson, “Battery performance models in ADVISOR,” *J. Power Sources*, vol.

110, no. 2, pp. 321–329, 2002.

[31] H. He, R. Xiong, and J. Fan, “Evaluation of lithium-ion battery equivalent circuit models for state of charge estimation by an experimental approach,” *Energies*, vol. 4, no. 4, pp. 582–598, 2011.

[32] F. M. González-longatt, “Circuit Based Battery Models : A Review,” *2Do Congr. Iberoam. Estud. Ing. Electr.*, p. , 2006.

[33] A.-I. Stan, M. Swierczynski, D.-I. Stroe, R. Teodorescu, S. J. Andreasen, and K. Moth, “A comparative study of lithium ion to lead acid batteries for use in UPS applications,” *Telecommun. Energy Conf. (INTELEC), 2014 IEEE 36th Int.*, pp. 1–8, 2014.

[34] I. Snihir, W. Rey, E. Verbitskiy, A. Belfadhel-Ayeb, and P. H. L. Notten, “Battery open-circuit voltage estimation by a method of statistical analysis,” *J. Power Sources*, vol. 159, no. 2, pp. 1484–1487, 2006.

[35] A. I. Stroe, M. Swierczynski, D. I. Stroe, and R. Teodorescu, “Performance model for high-power lithium titanate oxide batteries based on extended characterization tests,” *2015 IEEE Energy Convers. Congr. Expo. ECCE 2015*, pp. 6191–6198, 2015.

[36] A. Hentunen, T. Lehmuspelto, and J. Suomela, “Time-domain parameter extraction method for thevenin-equivalent circuit battery models,” *IEEE Trans. Energy Convers.*, vol. 29, no. 3, pp. 558–566, 2014.

[37] R. Jackey, M. Saginaw, P. Sanghvi, J. Gazzarri, T. Huria, and M. Ceraolo, “Battery Model Parameter Estimation Using a Layered Technique : An Example Using a Lithium Iron Phosphate Cell,” *MathWorks*, pp. 1–14, 2013.

[38] C. I. Ciontea, D. Sera, and F. Iov, “Influence of resolution of the input data on distributed generation integration studies,” *2014 Int. Conf. Optim. Electr. Electron. Equipment, OPTIM 2014*, pp. 673–680, 2014.

[39] C. Tang, M. Pathmanathan, W. L. Soong, and N. Ertugrul, “Effects of inertia on dynamic performance of wind turbines,” *2008 Australas. Univ. Power Eng. Conf.*, pp. 1–6, 2008.

[40] A. G. G. Rodríguez, A. G. Rodríguez, and M. B. Payán, “Key words,” vol. 1, no. 5, pp. 9–11, 2007.

[41] “Osiris Energy.” [Online]. Available: http://www.osirisenergy.com/.

[42] “Nordisk Folkecenter for vedvarende energi.” [Online]. Available: http://www.folkecenter.dk/dk/rd/vindkraft/smaa_vindmoller/godkendte-husstandsvindmoeller-i-danmark/.

[43] A. Universitet, “Modellering af husstandes.”

[44] LG, “LG NeON™ 72cell Module Cells.” [Online]. Available: http://www.lg.com/us/business/solar-panel/all-products/lg-LG360N2W-B3.